

Supporting Information For:

One-shot Multiple Borylation toward BN-Doped Nanographenes

*Kohei Matsui, Susumu Oda, Kazuki Yoshiura, Kiichi Nakajima, Nobuhiro Yasuda,
Takaji Hatakeyama**

Prof. T. Hatakeyama, K. Matsui, Dr. S. Oda, K. Yoshiura, K. Nakajima

Department of Chemistry, School of Science and Technology, Kwansei Gakuin University, 2-1
Gakuen, Sanda, Hyogo 669-1337, Japan

E-mail: hatake@kwansei.ac.jp

Dr. N. Yasuda

Japan Synchrotron Radiation Research Institute (JASRI), 1-1-1, Kouto, Sayo-cho, Sayo-gun, Hyogo,
679-5198, Japan

EXPERIMENTAL SECTION

General Procedure. All the reactions dealing with air- or moisture-sensitive compounds were carried out in a dry reaction vessel (Schlenk or round-bottomed flasks) connected to a Schlenk line equipped with an oil bubbler under a positive pressure of nitrogen. Air- and moisture-sensitive liquids and solutions were transferred *via* a syringe or a Teflon® cannula. Analytical thin-layer chromatography (TLC) was performed on glass plates coated with 0.25 mm 230–400 mesh silica gel containing a fluorescent indicator (Merck, #1.05715.0009). TLC plates were visualized by exposure to ultraviolet light (254 or 365 nm). Organic solutions were concentrated by rotary evaporation at *ca.* 10–50 mmHg. Flash column chromatography was performed on Merck silica gel 60 (spherical, neutral, 140–325 mesh) as described by Still et al.¹ Gel permeation chromatography was performed on a JAIGEL-1H and 2H (20 mm i.d.) with an LC-9130 (Japan Analytical Industry Co., Ltd.). Proton nuclear magnetic resonance (¹H NMR) and carbon nuclear magnetic resonance (¹³C NMR) spectra were recorded on JEOL ECX400 (400 MHz) NMR spectrometers or JEOL ECX500 (500 MHz) NMR spectrometers. Proton chemical shift values are reported in parts per million (ppm, δ scale) downfield from tetramethylsilane, and are referenced to the tetramethylsilane (δ 0), (CDCl₂)₂ (δ 6.00), or CDCl₃ (δ 7.26). ¹³C NMR spectra were recorded at 101 MHz or 126 MHz: carbon chemical shift values are reported in parts per million (ppm, δ scale) downfield from tetramethylsilane, and are referenced to the carbon resonance of tetramethylsilane (δ 0), (CDCl₂)₂ (δ 73.8), or CDCl₃ (δ 77.0). ¹¹B NMR spectra were recorded at 128 MHz or 160 MHz: boron chemical shift values are reported in parts per million (ppm, δ scale) and are referenced to the external standard boron signal of BF₃·Et₂O (CDCl₃, δ 0). ¹⁹F NMR spectra were recorded at 376 MHz or 470 MHz: fluorine chemical shift values are reported in parts per million (ppm, δ scale) and are referenced to the external standard fluorine signal of CF₃COOH (CDCl₃, δ -77.6). Data are presented as: chemical shift, multiplicity (s = singlet, d = doublet, t = triplet, q = quartet, quint = quintet, sext = sextet, sept = septet, m = multiplet and/or multiplet resonances, br = broad), coupling constant in hertz (Hz), signal area integration in natural numbers, and assignment (*italic*). IR spectra were recorded on an ATR-FTIR spectrometer (FT/IR-4200, JASCO or IRAffinith-1S, SHIMADZU). Characteristic IR absorptions are reported in cm⁻¹. Melting points were recorded on a Fisher-Jones Melting point Apparatus 12-144-1Q (according to the limitations of the apparatus, the compounds which did not melt up to 300 °C are presented as ">300 °C" after confirming that is not decomposed using NMR). Low-resolution mass spectra (LRMS) were obtained using the electron impact (EI) method with Shimadzu GCMS-QP2010 Ultra and the direct analysis in real time (DART) method with Ionsense SVP100 and JEOL JMS-T100LP and the matrix assisted laser desorption and ionization time-of-flight mass spectrometry (MALDI-TOF/MS) with JEOL JMS-S3000. High-resolution mass spectra (HRMS) were obtained using the EI method with JEOL JMS-T100LP and the DART method with Ionsense SVP100 and JEOL JMS-T100LP. UV-visible absorption spectra were measured by Shimazu UV-2600. Fluorescence spectra

were measured by HORIBA Scientific FluoroMax-4 or Hitachi High-Tech F-7000. Absolute PL quantum yields were recorded on a Hamamatsu Photonics C11347 or C9920-02G. Purity of isolated compounds was determined by ^1H NMR analyses. Sublimation was conducted by using ULVAC VPC-050 (10^1 – 10^{-3} Pa) prior to spectroscopic analysis.

Materials. Materials were purchased from Wako Pure Chemical Industries, Ltd. (Wako), Tokyo Chemical Industry Co., Ltd., Aldrich Inc. (Aldrich), and other commercial suppliers, and were used after appropriate purification, unless otherwise noted. Florisil® (100–200 mesh) was purchased from Kanto Chemical Co., Inc. (Kanto). N^1,N^1,N^3,N^3,N^5,N^5 -Hexaphenyl-1,3,5-benzenetriamine was purchased from Aldrich.

Solvent. Anhydrous solvents were purchased from above-described suppliers and/or dried over Molecular Sieves 4A (activation: heated by microwave apparatus and then dried *in vacuo*) and degassed before use. Water content of the solvent was determined with a Karl Fischer Moisture Titrator (AQ-2200, Hiranuma Sangyo Co., Ltd.) to be less than 20 ppm.

Computational Method. All calculations were performed with Gaussian 09 packages² unless otherwise noted. The DFT method was employed using the B3LYP hybrid functional.³ Structures were optimized with the 6-31G(d) basis set.⁴ The time-dependent density functional theory (TD-DFT) calculation⁵ was conducted at the B3LYP/6-311+G(d,p) level after the geometry optimization at the B3LYP/6-31G(d) level (B3LYP/6-311+G(d,p)//B3LYP/6-31G(d)). Nucleus independent chemical shifts (NICS) were evaluated by using the gauge invariant atomic orbital⁶ (GIAO) approach at the GIAO-B3LYP/6-311+G(d,p)//B3LYP/6-31G(d) level.

Summary of DFT calculation

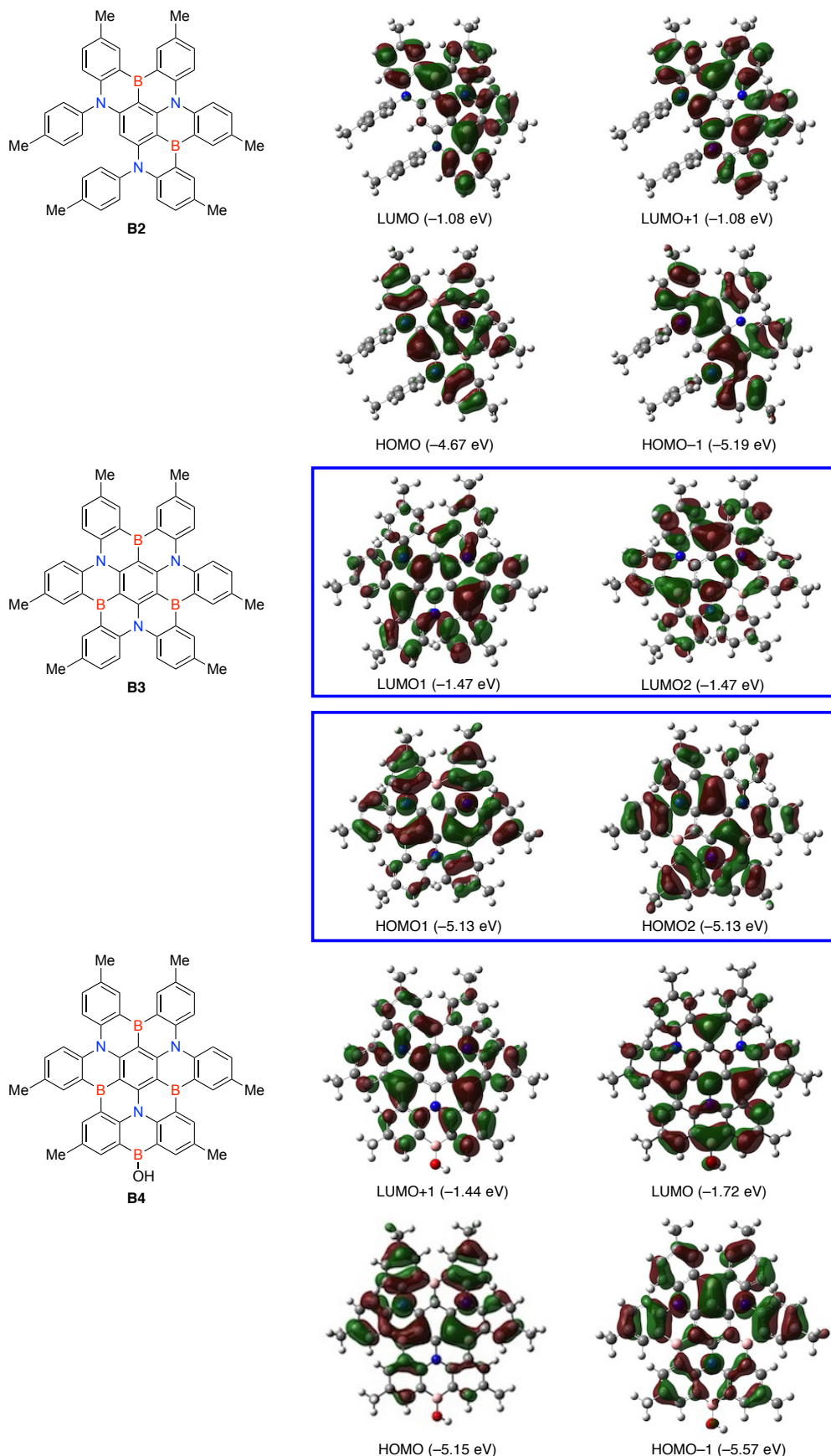


Figure S1. Kohn–Sham frontier orbitals of **B2**, **B3** and **B4** calculated at the B3LYP/6-31G(d) level of theory. Degenerate orbitals are shown in a blue square.

Table S1. Summary of TD-DFT calculation for B2, B3 and B4 at the S₀ structure at the B3LYP/6-311+G(d,p)//B3LYP/6-31G(d) level and related photophysical data.

compound	calculation				experiment				
	transition	wavelength (nm)	energy (eV)	oscillator strength	λ_{ab}^a (nm)	λ_{em}^a (nm)	λ_{ab}^b (nm)	λ_{em}^b (nm)	ε^b (L mol ⁻¹ cm ⁻¹)
B2	S ₀ –S ₁	416.68	2.9755	0.0621	438	455	433	461	4.0 x 10 ⁴
	S ₀ –S ₂	412.09	3.0087	0.2220					
	S ₀ –S ₃	354.13	3.5011	0.0072					
B3	S ₀ –S ₁	425.84	2.9115	0.0006	430	441	430	442	5.1 x 10 ³
	S ₀ –S ₂	407.69	3.0411	0					
	S ₀ –S ₃	380.80	3.2559	0.5200	396	—	396	—	5.5 x 10 ⁴
	S ₀ –S ₄	380.78	3.2560	0.5200					
B4	S ₀ –S ₁	436.38	2.8412	0.0801	440	450	440	449	1.7 x 10 ⁴
	S ₀ –S ₂	418.84	2.9602	0.1021					
	S ₀ –S ₃	392.22	3.1611	0.1139					

^a In a PMMA film (1wt%). ^b In CH₂Cl₂ (0.02 mM).

compound	transition	coefficient of orbital			
B2	S ₀ –S ₁	HOMO – LUMO (0.69572)			
	S ₀ –S ₂	HOMO – LUMO+1 (0.66114)	HOMO–1 – LUMO (0.22320)		
	S ₀ –S ₃	HOMO – LUMO+2 (0.57435)	HOMO–1 – LUMO+1 (0.34117)	HOMO–2 – LUMO (-0.19610)	
B3	S ₀ –S ₁	HOMO2 – LUMO1 (0.48140)	HOMO1 – LUMO2 (-0.48122)	HOMO1 – LUMO1 (-0.12270)	HOMO2 – LUMO2 (0.12262)
	S ₀ –S ₂	HOMO1 – LUMO1 (0.48170)	HOMO2 – LUMO2 (0.48124)	HOMO2 – LUMO1 (0.12271)	HOMO1 – LUMO2 (-0.12269)
	S ₀ –S ₃	HOMO2 – LUMO2 (0.43311)	HOMO1 – LUMO1 (-0.43264)		
	S ₀ –S ₄	HOMO1 – LUMO2 (0.43295)	HOMO2 – LUMO1 (0.43278)		
B4	S ₀ –S ₁	HOMO – LUMO (0.63525)			
	S ₀ –S ₂	HOMO–1 – LUMO (0.66000)	HOMO – LUMO+1 (0.20854)		
	S ₀ –S ₃	HOMO – LUMO+1 (0.50700)	HOMO – LUMO+2 (-0.30849)	HOMO–1 – LUMO+2 (-0.20563)	HOMO–1 – LUMO (-0.17925)
		HOMO – LUMO (-0.15897)	HOMO–2 – LUMO (-0.15504)	HOMO–1 – LUMO+1 (-0.11622)	

A representative procedure for electrophilic C–H borylation shown in Table S2

To a Schlenk tube were added **1** (66.4 mg, 0.10 mmol), boron triiodide (0.478 g, 1.2 mmol) and 1,2-dichlorobenzene (1.0 mL) at room temperature under a nitrogen atmosphere. After stirring at 200 °C for 12 h, the reaction mixture was allowed to cool to room temperature. After phosphorus buffer solution (pH 7, 20 mL) was added to the reaction mixture, the aqueous layer was separated and extracted with dichloromethane (60 mL, three times). The combined organic layers were concentrated *in vacuo*. The yield of the **B4** in the crude product was determined by ¹H NMR using 1,1,2,2-tetrachloroethane as an internal standard.

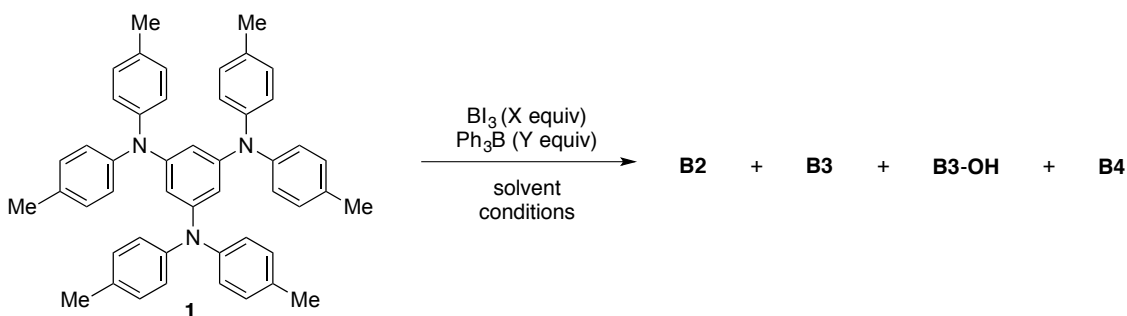


Table S2

entry ^a	X	Y	solvent	conditions	yield ^b			
					B2	B3	B3-OH	B4
1	5.0	2.0	1,2-dichlorobenzene	180 °C, 20 h	41%	0%	0%	0%
2	5.0	0	1,2-dichlorobenzene	180 °C, 20 h	65%	0%	0%	0%
3	5.0	2.0	1,2-dichlorobenzene	190 °C, 20 h	80% (76%)	0%	0%	0%
4 ^{d,e}	5.0	2.0	1,2-dichlorobenzene	190 °C, 20 h	0%	0%	0%	0%
5	5.0	0	1,2-dichlorobenzene	190 °C, 20 h	0%	0%	20%	21%
6	5.0	2.0	1,2,4-trichlorobenzene	190 °C, 20 h	35%	33%	9%	0%
7	5.0	0	1,2,4-trichlorobenzene	190 °C, 20 h	16%	13%	36%	0%
8 ^f	5.0	2.0	1,2,4-trichlorobenzene	200 °C, 20 h	6%	48% (45%)	0%	0%
9	5.0	0	1,2,4-trichlorobenzene	200 °C, 20 h	14%	30%	24%	6%
10	5.0	2.0	1,2,4-trichlorobenzene	210 °C, 20 h	0%	40%	0%	3%
11	5.0	0	1,2,4-trichlorobenzene	210 °C, 20 h	0%	34%	2%	11%
12	5.0	2.0	1,2,4-trichlorobenzene	220 °C, 20 h	0%	40%	0%	0%
13	5.0	0	1,2,4-trichlorobenzene	220 °C, 20 h	0%	35%	0%	0%
14	12	0	1,2-dichlorobenzene	180 °C, 20 h	30%	7%	0%	0%
15	12	0	1,2-dichlorobenzene	190 °C, 20 h	0%	3%	0%	14%
16	12	0	1,2,4-trichlorobenzene	190 °C, 20 h	16%	8%	18%	4%
17	12	0	1,2-dichlorobenzene	200 °C, 12 h	0%	3%	0%	41% (35%)
18 ^d	12	0	1,2-dichlorobenzene	200 °C, 12 h	0%	0%	0%	0%
19	12	0	1,2-dichlorobenzene	200 °C, 20 h	0%	1%	0%	33%
20	12	0	1,2,4-trichlorobenzene	200 °C, 20 h	0%	4%	0%	8%
21	12	0	1,2-dichlorobenzene	210 °C, 20 h	0%	0%	0%	7%
22	12	0	1,2,4-trichlorobenzene	210 °C, 20 h	0%	2%	0%	5%

^aReactions were carried out on a 0.10 mmol scale in a Schlenk tube under a nitrogen atmosphere. ^bYields were determined by ¹H NMR analysis using 1,1,2,2-tetrachloroethane as an internal standard. Recovery of **1** was not observed in all the entries. ^cIsolated yield. ^dReactions were carried out in an autoclave. ^eDi-*p*-tolylamine (4% yield) was detected by GC analysis. ^fReactions were carried out on a 1.0 mmol scale in a flask under a nitrogen atmosphere.

A representative procedure for electrophilic C–H borylation shown in Table S3

To a Schlenk tube were added **1** (66.4 mg, 0.10 mmol), boron triiodide (0.196 g, 0.50 mmol), triphenylborane (48.4 mg, 0.20 mmol) and 2,4-dichlorotoluene (1.0 mL) at room temperature under a nitrogen atmosphere. After stirring at 210 °C for 20 h, the reaction mixture was allowed to cool to room temperature. After addition of *N,N*-diisopropylethylamine (0.26 mL, 1.5 mmol), the solvent was removed *in vacuo*. The yield of **B3** in the crude product was determined by ¹H NMR using 1,1,2,2-tetrachloroethane as an internal standard.

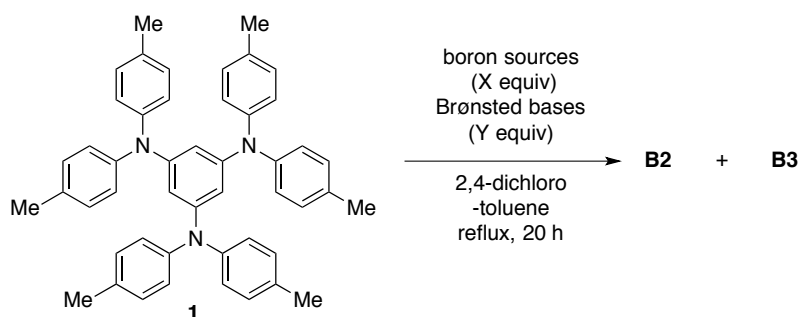


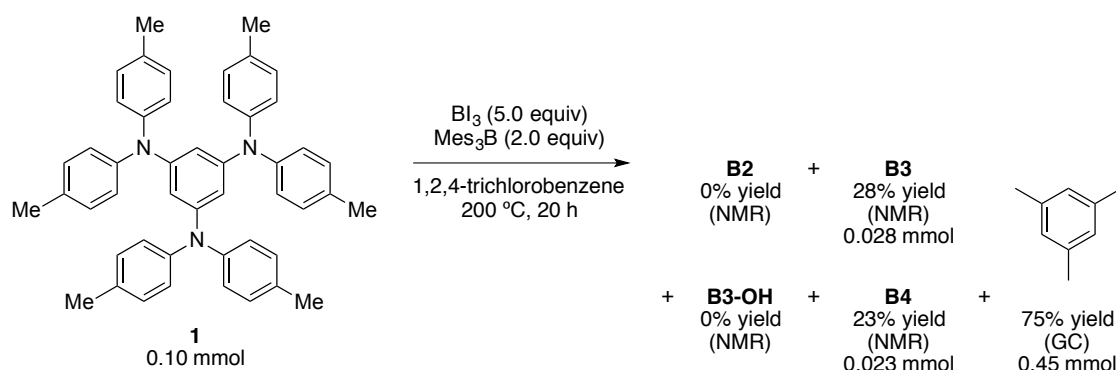
Table S3

entry ^a	boron sources	X	Brønsted bases	Y	yield ^b		
					recovery	B2	B3
1	BCl ₃	5.0	none	—	73%	0%	0%
2	BBr ₃	5.0	none	—	0%	44%	0%
3	Bi ₃	5.0	none	—	0%	0%	13%
4	BBBr ₃	5.0	BPh ₃	2.0	0%	36%	0%
5	Bi ₃	5.0	BPh ₃	2.0	0%	0%	30%
6	Bi ₃	5.0	EtN <i>i</i> Pr ₂	2.0	0%	54%	0%
7	Bi ₃	5.0	<i>N,N</i> -dimethyltoluidine	2.0	0%	44%	0%

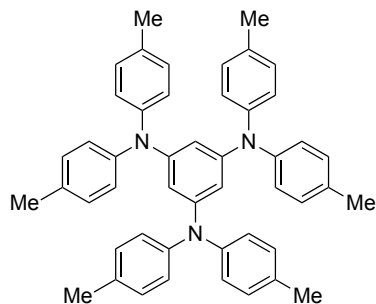
^aReactions were carried out on a 0.10 mmol scale in a Schlenk tube under a nitrogen atmosphere. ^bYields were determined by ¹H NMR analysis using 1,1,2,2-tetrachloroethane as an internal standard.

A procedure for electrophilic C–H borylation using Mes₃B as a Brønsted base

To a Schlenk tube were added **1** (66.4 mg, 0.10 mmol), boron triiodide (0.196 g, 0.50 mmol), trimesitylborane (73.7 mg, 0.20 mmol) and 1,2,4-trichlorobenzene (1.0 mL) at room temperature under a nitrogen atmosphere. After stirring at 200 °C for 20 h, the reaction mixture was allowed to cool to room temperature. After phosphorus buffer solution (pH 7, 20 mL) was added to the reaction mixture, the aqueous layer was separated and extracted with dichloromethane (60 mL, three times). The combined organic layers were concentrated *in vacuo*. The yield of the compounds in the crude product were determined by gas chromatography using dodecane as an internal standard and ¹H NMR using 1,1,2,2-tetrachloroethane as an internal standard.

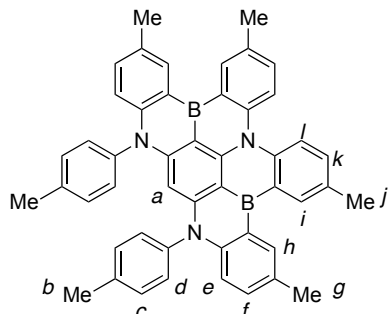


Synthesis of *N¹,N¹,N³,N³,N⁵,N⁵-hexakis(4-methylphenyl)-1,3,5-benzenetriamine (1)*



Di-*p*-tolylamine (18.9 g, 96 mmol), sodium *tert*-butoxide (11.5 g, 0.12 mol), tri-*tert*-butyl phosphine (60.7 mg, 0.30 mmol), tris(dibenzylideneacetone)dipalladium(0) (0.137 g, 0.15 mmol) and 1,3,5-tribromobenzene (9.44 g, 30 mmol) were dissolved in toluene (300 mL) under a nitrogen atmosphere. After stirring at 60 °C for 7 h, the reaction mixture was filtered with a pad of Florisil®(eluent: toluene). After the solvent was removed *in vacuo*, the crude product was washed with methanol by using a sonicator to obtain the title compound (23.8 g, 98% yield, >99% pure on NMR analysis) as a white solid. Analytical data for the titled compound have been reported.⁷

Synthesis of 3,6,14,17-tetramethyl-9,11-di-*p*-tolyl-9,11-dihydro-9,11,19b-triaza-4b,15b-diborabenzo[3,4]phenanthro[2,1,10,9-fghi]pentacene (B2)

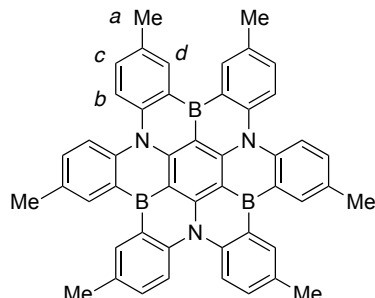


To a Schlenk tube were added **1** (66.4 mg, 0.10 mmol), boron triiodide (0.196 g, 0.50 mmol), triphenylborane (48.4 mg, 0.20 mmol) and 1,2-dichlorobenzene (1.0 mL) at room temperature under a nitrogen atmosphere. After stirring at 190 °C for 20 h, the reaction mixture was allowed to cool to room temperature. After phosphorus buffer solution (pH 7, 20 mL) was added to the reaction mixture, the aqueous layer was separated and extracted with dichloromethane (60 mL, three times). The combined organic layers were concentrated *in vacuo*. The yield of the title compound in the crude product was determined to be 80% by ¹H NMR using 1,1,2,2-tetrachloroethane as an internal standard. The crude product was washed with acetonitrile by using a sonicator to obtain the title compound (51.6 mg, 76% yield, 98% pure on NMR analysis) as a yellow solid. IR (neat): cm⁻¹ 3024 (Ar-H), 2970, 2916, 2857, 1572, 1412, 1314, 1250, 816, 808, 729; mp: >300 °C; ¹H NMR (400 MHz, CDCl₃) δ 2.45 (s, 6H, *b*), 2.56 (s, 6H, *g*), 2.58 (s, 6H, *j*), 5.24 (s, 1H, *a*), 6.74 (d, *J* = 8.7 Hz, 2H, *e*), 6.94 (d, *J* = 7.9 Hz, 4H, *d*), 7.15–7.25 (m, 6H, *c,f*), 7.34 (dd, *J* = 1.8, 8.7 Hz, 2H, *k*), 8.18 (d, *J* = 8.7 Hz, 2H,

l), 8.58 (d, *J* = 1.8 Hz, 2H, *i*), 8.67 (d, *J* = 1.6 Hz, 2H, *h*); ¹³C NMR (101 MHz, CDCl₃) δ 20.2 (2C), 21.3 (2C), 21.3 (2C), 93.1 (1C), 116.7 (2C), 123.7 (2C), 129.1 (2C), 129.7 (4C), 130.6 (2C), 131.1 (2C), 131.9 (4C), 132.2 (2C), 134.1 (2C), 134.5 (2C), 137.7 (2C), 139.3 (2C), 144.7 (2C), 145.7 (2C), 146.6 (1C), 149.6 (2C). The NMR signal of the carbon α to the boron was not observed.; ¹¹B NMR (128 MHz, CDCl₃) δ 37.8; HRMS (DART) *m/z* [M+H]⁺ calcd for C₄₈H₄₀B₂N₃ 680.3424; observed 680.3404.

To a two necked round-bottomed flask equipped with a reflux condenser were added **1** (0.332 g, 0.50 mmol), boron triiodide (0.979 g, 2.5 mmol), triphenylborane (0.242 g, 1.0 mmol) and 1,2-dichlorobenzene (5.0 mL) at room temperature under a nitrogen atmosphere. After stirring at 190 °C for 20 h, the reaction mixture was allowed to cool to room temperature. After addition of *N,N*-diisopropylethylamine (1.31 mL, 7.5 mmol), the solvent was removed *in vacuo*. The yield of the title compound in the crude product was determined to be 73% by ¹H NMR using 1,1,2,2-tetrachloroethane as an internal standard. The crude product was washed with acetonitrile and ethyl acetate to obtain the title compound (0.241 g, 71% yield, 99% pure on NMR analysis) as a yellow solid.

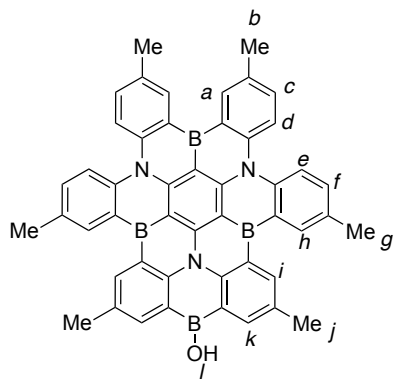
Synthesis of 2,7,10,15,18,23-hexamethyl-4b,12b,20b-triaza-8b,16b-24b-triborahexabenzo [*a,d,g,j,m,p*]coronene (**B3**)



To a two necked round-bottomed flask equipped with a reflux condenser were added **1** (0.664 g, 1.0 mmol), boron triiodide (1.96 g, 5.0 mmol), triphenylborane (0.484 g, 2.0 mmol) and 1,2,4-trichlorobenzene (10 mL) at room temperature under a nitrogen atmosphere. After stirring at 200 °C for 20 h, the reaction mixture was allowed to cool to room temperature. After phosphorus buffer solution (pH 7, 200 mL) was added to the reaction mixture, the aqueous layer was separated and extracted with dichloromethane (600 mL, three times). The combined organic layers were concentrated *in vacuo*. The yield of the title compound in the crude product was determined to be 48% by ¹H NMR using 1,1,2,2-tetrachloroethane as an internal standard. The crude product was washed with acetonitrile by using a sonicator to obtain the title compound (0.296 g, 43% yield, 98% pure on NMR analysis) as a yellow solid. The filtrate was purified by GPC (eluent: 1,2-dichloroethane) to obtain the title compound (15.8 mg, 2.3% yield, >98% pure on NMR analysis) as

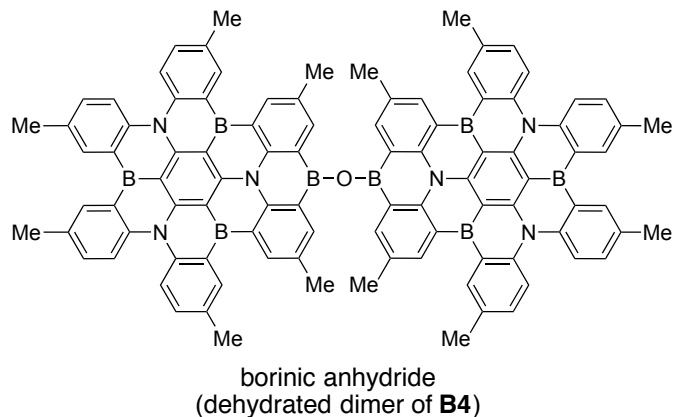
a yellow solid. The total yield was 45% (0.312 g, >98% pure on NMR analysis). IR (neat): cm^{-1} 3021 (Ar-H), 2934, 2913, 2857, 1572, 1531, 1410, 1383, 1373, 1321, 1298, 1236, 1219, 1152, 820; mp: >300 °C; ^1H NMR (400 MHz, $\text{CDCl}_3/\text{CS}_2 = 1/3$) δ 2.63 (s, 18H, *a*), 7.40 (dd, *J* = 1.8, 8.5 Hz, 6H, *c*), 8.19 (d, *J* = 8.5 Hz, 6H, *b*), 8.62 (d, *J* = 1.8 Hz, 6H, *d*); ^{13}C NMR (101 MHz, $\text{CDCl}_3/\text{CS}_2 = 1/3$) δ 21.2 (6C), 123.6 (6C), 130.2 (6C), 132.7 (6C), 133.8 (6C), 144.6 (6C). The NMR signal of the carbon α to the boron and center of benzene was not observed. ^{11}B NMR (128 MHz, $\text{CDCl}_3/\text{CS}_2 = 1/3$) δ 38.9; HRMS (DART) *m/z* [M+H]⁺ calcd for $\text{C}_{48}\text{H}_{37}\text{B}_3\text{N}_3$ 688.3288; observed 688.3267.

Synthesis of 2,5,10,13,18,21-hexamethyl-23*H*-3a²,7b,15b-triaza-3b,11b,19b,23-tetraboradinaphtho[1,2,3,4-*fg*:1',2',3',4'-*pqr*]phenaleno[1,2,3,4,5-za₁b₁c₁d₁]trinaphthylen-23-ol (B4**)**

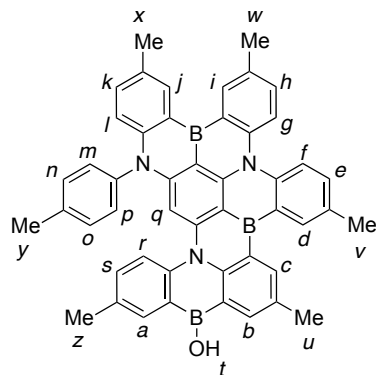


To a Schlenk tube were added **1** (66.4 mg, 0.10 mmol), boron triiodide (0.478 g, 1.2 mmol) and 1,2-dichlorobenzene (1.0 mL) at room temperature under a nitrogen atmosphere. After stirring at 200 °C for 12 h, the reaction mixture was allowed to cool to room temperature. After phosphorus buffer solution (pH 7, 20 mL) was added to the reaction mixture, the aqueous layer was separated and extracted with dichloromethane (60 mL, three times). The combined organic layers were concentrated *in vacuo*. The yield of the title compound in the crude product was determined to be 41% by ^1H NMR using 1,1,2,2-tetrachloroethane as an internal standard. The crude product was purified by GPC (eluent: 1,2-dichloroethane) to obtain the title compound (25.0 mg, 35% yield, 97% pure on NMR analysis) as a yellow solid, containing 3% of the corresponding borinic anhydride (dehydrated dimer of the title compound, see Figure S18). The title compound was further purified as follows: The solution of the title compound in THF (5.0 mL) and water (1.0 mL) was stirred at 60 °C for 2 h. After dilution with an excess amount of water, the resulting precipitate was filtered and washed with water to give the title compound with >98% purity on NMR analysis. The spectroscopic measurements were conducted just after hydrolysis because 3% of the borinic anhydride again formed during removal of volatiles *in vacuo*. Figure S19 shows ^1H NMR spectrum after heating of the NMR sample of **B4** at 60 °C for 2 h in $(\text{CDCl}_2)_2$ with D_2O . IR (neat): cm^{-1} 3022 (Ar-H), 2918, 2856, 1611, 1576, 1533, 1418, 1381, 1296, 1240, 1155, 819, 735; mp: >300 °C; ^1H NMR (500 MHz, $(\text{CDCl}_2)_2$) δ 2.60

(s, 6H, *b*), 2.69 (s, 6H, *g*), 2.80 (s, 6H, *j*), 5.80 (brs, 1H, *l*), 7.40 (d, *J* = 8.6 Hz, 2H, *f*), 7.47 (d, *J* = 8.6 Hz, 2H, *c*), 8.15 (d, *J* = 8.6 Hz, 2H, *e*), 8.24 (d, *J* = 8.6 Hz, 2H, *d*), 8.36 (s, 2H, *h*), 8.48 (d, *J* = 2.3 Hz, 2H, *k*), 8.64 (s, 2H, *a*), 9.06 (d, *J* = 2.3 Hz, 2H, *i*); ¹³C NMR (101 MHz, (CDCl₂)₂) δ 20.5 (2C), 21.1 (2C), 21.2 (2C), 110.4 (2C), 111.6 (2C), 123.2 (1C), 123.4 (2C), 123.7 (2C), 123.8 (2C), 127.0 (2C), 129.6 (2C), 130.1 (2C), 130.5 (2C), 131.6 (2C), 133.0 (2C), 133.6 (2C), 134.8 (2C), 135.3 (2C), 140.7 (2C), 143.9 (2C), 144.9 (2C), 147.6 (2C), 149.8 (2C). The NMR signal of the carbon α to the boron was not observed. ¹¹B NMR (128 MHz, (CDCl₂)₂) δ 39.5; HRMS (MALDI-TOF/MS) *m/z* [M]⁺ calcd for C₄₈H₃₅B₄N₃O 713.3152; observed 713.3147.



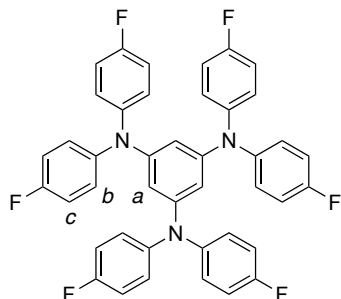
Synthesis of 3,6,10,17-pentamethyl-14-*p*-tolyl-8,14-dihydro-12*b*,14,22*b*-triaza-4*b*,8,18*b*-triborabenzo[3,4]phenanthro[2,1,10,9-*fghi*]naphtho[3,2,1-*opq*]pentacene-8-ol (**B3-OH**)



The title compound was isolated as a yellow solid from the combined crude products obtained during the screening of the reaction conditions (Table S1, entries 4 and 6). IR (neat): cm⁻¹ 3028 (Ar-H), 3015, 2945, 2920, 2854, 2729, 2359, 1900, 1732, 1722, 1611, 1587, 1548, 1508, 1489, 1454, 1410, 1379, 1300, 1252, 1215, 1182, 1144, 1128, 1092, 1034, 968, 883, 868, 812, 777, 760, 727, 653, 621, 611; mp: 275 °C; ¹H NMR (500 MHz, (CDCl₂)₂) δ 2.46 (s, 3H, *z*), 2.48 (s, 3H, *y*), 2.61 (s, 3H, *u*), 2.63 (m, 6H, *v* and *w*), 2.66 (s, 3H, *x*), 6.77 (s, 1H, *q*), 6.89 (d, *J* = 8.6 Hz, 1H, *l*), 7.08 (d, *J* = 7.45 Hz, 1H, *p*), 7.13 (d, *J* = 8.6 Hz, 1H, *s*), 7.31–7.40 (m, 4H, *o,m,k,e*), 7.46 (d, *J* = 8.6 Hz, 1H, *h*), 7.55 (d, *J* = 7.45 Hz, 1H, *n*), 7.75 (s, 1H, *a*), 7.81 (d, *J* = 8.6 Hz, 1H, *r*), 8.03 (s, 1H, *b*), 8.17 (d, *J* = 8.6 Hz, 1H, *f*), 8.26 (d, *J* = 8.6 Hz, 1H, *g*), 8.39 (s, 1H, *i*), 8.64–8.65 (m, 2H, *c* and *j*), 8.77 (s, 1H, *d*); ¹³C NMR (101 MHz,

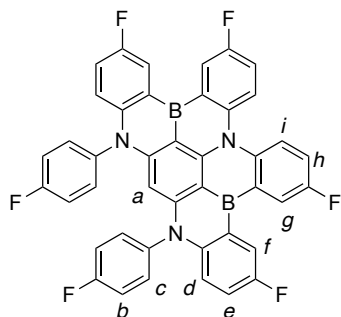
(CDCl₂) δ 20.7 (1C), 21.0 (1C), 21.1 (1C), 21.2 (1C), 21.2 (1C), 21.3 (1C), 98.7 (1C), 99.4 (1C), 111.6 (1C), 113.3 (1C), 117.5 (1C), 121.7 (1C), 122.8 (1C), 123.2 (1C), 123.7 (1C), 123.9 (1C), 126.2 (1C), 126.3 (1C), 129.4 (1C), 129.5 (1C), 129.8 (1C), 129.9 (1C), 130.3 (1C), 130.3 (1C), 130.5 (1C), 131.3 (1C), 131.3 (1C), 131.5 (1C), 132.0 (1C), 132.4 (1C), 132.5 (1C), 133.0 (1C), 133.5 (1C), 133.7 (1C), 134.3 (1C), 134.3 (1C), 138.3 (1C), 138.9 (1C), 139.2 (1C), 144.2 (1C), 144.7 (1C), 144.9 (1C), 145.5 (1C), 146.4 (1C), 148.2 (1C), 148.3 (1C), 148.9 (1C). The NMR signal of the carbon α to the boron was not observed.; ¹¹B NMR (128 MHz, (CDCl₂) δ 36.8; HRMS (MALDI-TOF/MS) *m/z* [M]⁺ calcd for C₄₈H₃₈B₃N₃O 705.3294; observed 705.3231.

Synthesis of *N^{1,N^{1,N^{3,N^{3,N^{5,N^{5-hexakis(4-fluorophenyl)-1,3,5-benzenetriamine (1-F)}}}}}}*



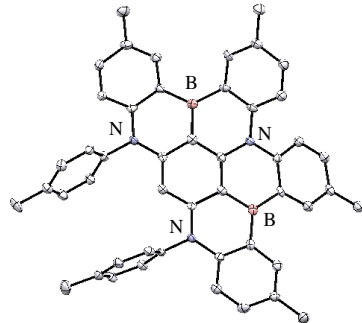
4,4'-Difluorodiphenylamine (3.28 g, 16.0 mmol), potassium *tert*-butoxide (2.24 g, 20.0 mmol), tri-*tert*-butyl phosphine (0.101 g, 0.50 mmol), tris(dibenzylideneacetone)dipalladium(0) (0.229 g, 0.25 mmol) and 1,3,5-tribromobenzene (1.57 g, 5.0 mmol) were dissolved in toluene (40 mL) under a nitrogen atmosphere. After stirring at 100 °C for 20 h, the reaction mixture was filtered with a pad of Florisil®(eluent: dichloromethane). After the solvent was removed *in vacuo*, the crude product was washed with methanol by using a sonicator to obtain the title compound (2.84 g, 82% yield, >99% pure on NMR analysis) as a white solid. IR (neat): cm⁻¹ 3059 (Ar-H), 1598, 1580, 1500, 1470, 1305, 1288, 1253, 1217, 1147, 1096, 1039, 1010, 829, 798, 709, 692, 638; mp: 254 °C; ¹H NMR (400 MHz, CDCl₃) δ 6.11 (s, 1H, *a*), 6.85–6.90 (m, 12H, *b*), 6.92–6.96 (m, 12H, *c*); ¹³C NMR (101 MHz, CDCl₃) δ 110.2 (3C), 115.9 (d, *J*_{C-F} = 22.0 Hz 12C), 125.8 (d, *J*_{C-F} = 8.6 Hz, 12C), 143.2 (d, *J*_{C-F} = 2.9 Hz 6C), 149.3 (3C), 158.8 (d, *J*_{C-F} = 242.5 Hz, 6C); ¹¹F NMR (376 MHz, CDCl₃) δ -119.6; HRMS (DART) *m/z* [M+H]⁺ calcd for C₄₂H₂₈F₆N₃ 688.6974; observed 688.6995.

Synthesis of 3,6,14,17-tetrafluoro-9,11-di-p-fluorophenyl-9,11-dihydro-9,11,19b-triaza-4b,15b-diborabenzo[3,4]phenanthro[2,1,10,9-fghi]pentacene (B2-F)

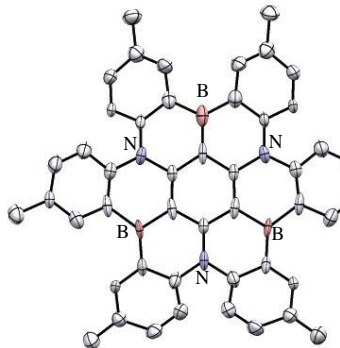


To a two necked round-bottomed flask equipped with a reflux condenser were added **1-F** (0.138 g, 0.20 mmol), boron triiodide (0.391 g, 1.0 mmol), triphenylborane (96.7 mg, 0.40 mmol) and 1,2-dichlorobenzene (5.0 mL) at room temperature under a nitrogen atmosphere. After stirring at 200 °C for 20 h, the reaction mixture was allowed to cool to room temperature. After addition of *N,N*-diisopropylethylamine (0.52 mL, 3.0 mmol), the solvent was removed *in vacuo*. The yield of the title compound in the crude product was determined to be 64% by ¹H NMR using 1,1,2,2-tetrachloroethane as an internal standard. The crude product was washed with acetonitrile to obtain the title compound (81.9 mg, 58% yield, 98% pure on NMR analysis) as a yellow solid. IR (neat): cm⁻¹ 3076 (Ar-H), 1583, 1462, 1359, 1251, 839, 808, 731; mp: >300 °C; ¹H NMR (500 MHz, (CDCl₂)₂) δ 5.10 (s, 1H, *a*), 6.87 (dd, *J* = 4.5, 9.0 Hz, 2H, *d*), 7.14–7.35 (m, 12H, *b, c, e, h*), 8.23 (dd, *J* = 4.5, 9.5 Hz, 2H, *i*), 8.38 (dd, *J* = 3.0, 9.0 Hz, 2H, *g*), 8.46 (dd, *J* = 3.0, 9.0 Hz, 2H, *f*); ¹³C NMR (101 MHz, (CDCl₂)₂) δ 92.6 (2C), 93.2 (1C), 93.7 (2C), 99.5 (1C), 110.4 (2C), 116.3–119.2 (m, 6C), 124.6 (2C), 125.7 (dd, *J*_{C-F} = 7.2, 20.4 Hz 2C), 131.2 (2C), 131.7 (2C), 132.1 (2C), 137.4 (2C), 142.9 (2C), 143.7 (2C), 146.8 (2C), 149.9 (4C), 157.5 (d, *J*_{C-F} = 242.3 Hz 2C), 158.9 (d, *J*_{C-F} = 245.9 Hz 2C), 162.4 (d, *J*_{C-F} = 254.3 Hz 2C); ¹¹B NMR (128 MHz, (CDCl₂)₂) δ 37.2; ¹⁹F NMR (376 MHz, (CDCl₂)₂) δ -123.0, -119.0, -112.3; HRMS (DART) *m/z* [M+H]⁺ calcd for C₄₈H₄₀B₂N₃ 704.1888; observed 704.1918.

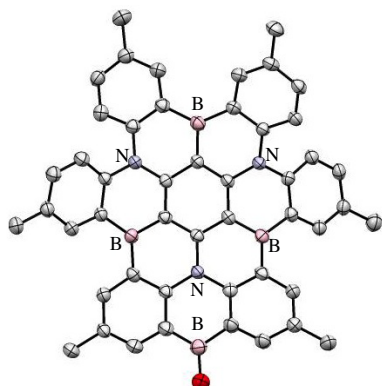
Crystallographic Data Collection and Structure Determination. The crystal data of **B2**, **B3** and **B4** were collected at the BL40XU beamline of the SPring-8 using an ADSC Quantum 315 CCD detector and Si(111)-monochromated X-ray radiation (**B2**: $\lambda = 0.78202$ Å, **B3**: $\lambda = 0.78207$ Å, **B4**: $\lambda = 0.78130$ Å). The reflection data for **B2**, **B3** and **B4** were integrated, scaled, and averaged by using Rigaku Process-auto software. Semi-empirical absorption correction was applied using the program of Abscor.⁸ The structures were solved by a direct method (SIR2004⁹ or SIR2008¹⁰) and refined by full-matrix least square method on F^2 for all reflections (SHELXL-97 or SHELXS-2013¹¹). All hydrogen atoms were placed using AFIX instructions (C–H = 0.95 Å), while all other atoms were refined anisotropically. In the subsequent refinement, the function $\sum w(F_o^2 - F_c^2)^2$ was minimized, where $|F_o|$ and $|F_c|$ are the observed and calculated structure factor amplitudes, respectively. The agreement indices are defined as $R_1 = \sum(|F_o| - |F_c|)/\sum|F_o|$ and $wR_2 = [\sum w(F_o^2 - F_c^2)^2 / \sum(wF_o^4)]^{1/2}$. All calculations were performed by using Rigaku CrystalStructure 4.1 or Yadokari-XG 2009 and illustrations were drawn by using ORTEP-3.



Formula	$C_{48}H_{39}B_2N_3, 1.5(C_6H_4Cl_2), 0.5(C_6H_{14})$	Abs. Coefficient, cm^{-1}	0.9991
Formula Weight	941.00	F(000)	984
Temperature, K	100	Crystal Size, mm^3	0.10, 0.10, 0.10
Wavelength, \AA	0.78202	$2\theta_{\min}, 2\theta_{\max}, \text{deg}$	1.51, 27.50
Crystal System	Triclinic	Index Ranges	$-13 \leq h \leq 13$
Space Group	$P\bar{1}$ (No.2)		$-17 \leq k \leq 17$
$a, \text{\AA}$	11.1700(6)	Reflections (unique)	8329
$b, \text{\AA}$	14.8457(9)	Reflections ($I > 2.0\sigma(I)$)	5856
$c, \text{\AA}$	15.0390(8)	Parameters	674
α, deg	89.159(2)	GOF on F^2	1.107
β, deg	76.8926(18)	$R_l (I > 2.0\sigma(I))$	0.0482
γ, deg	89.868(2)	R, wR_2 (all data)	0.0820, 0.1176
Volume, \AA^3	2428.6(2)	Largest diff peak and hole, $e, \text{\AA}^{-3}$	0.323, -0.352
Z	2		
Density _{calcd} , g · cm^{-3}	1.330		



Formula	$C_{48}H_{36}B_3N_3$	F(000)	1440
Formula Weight	687.23	Crystal Size, mm^3	0.30, 0.20, 0.05
Temperature, K	100(2)	$2\theta_{\min}, 2\theta_{\max}, \text{deg}$	2.42, 27.50
Wavelength, \AA	0.78207	Index Ranges	$-13 \leq h \leq 13$
Crystal System	Monoclinic		$-18 \leq k \leq 18$
Space Group	$C 2/c$ (No.15)	Reflections (unique)	2936
$a, \text{\AA}$	11.421(7)	Reflections ($I > 2.0\sigma(I)$)	1881
$b, \text{\AA}$	16.021(9)	Parameters	260
$c, \text{\AA}$	18.801(11)	GOF on F^2	1.300
β, deg	94.537(4)	$R_l (I > 2.0\sigma(I))$	0.1294
Volume, \AA^3	3429(3)	R, wR_2 (all data)	0.1680, 0.3227
Z	4	Largest diff peak and hole, $e, \text{\AA}^{-3}$	1.056, -0.477
Density _{calcd} , g · cm^{-3}	1.331	Abs. Coefficient, cm^{-1}	0.092



Formula	$C_{48}H_{35}B_4N_3O, 1.74(C_2H_3N)$	F(000)	820
Formula Weight	784.33	Crystal Size, mm^3	0.05, 0.02, 0.01
Temperature, K	100(2)	$2\theta_{\min}, 2\theta_{\max}, \text{deg}$	2.64, 27.500
Wavelength, \AA	0.78130	Index Ranges	$-14 \leq h \leq 14$
Crystal System	Triclinic		$-14 \leq k \leq 14$
Space Group	$P\bar{1}$ (No.2)	Reflections (unique)	6753
$a, \text{\AA}$	12.2055(6)	Reflections ($I > 2.0\sigma(I)$)	4285
$b, \text{\AA}$	12.6188(7)	Parameters	570
$c, \text{\AA}$	14.2094(8)	GOF on F^2	1.405
α, deg	108.697(4)	$R_l (I > 2.0\sigma(I))$	0.0666
β, deg	105.730(4)	R, wR_2 (all data)	0.1126, 0.1770
γ, deg	91.432(4)	Largest diff peak and hole, $e, \text{\AA}^{-3}$	0.520, -0.345
Volume, \AA^3	1980(19)		
Z	2		
Density _{calcd} , g · cm^{-3}	1.315		
Abs. Coefficient, cm^{-1}	0.094		

Figure S2. X-ray crystal structures of **B2**, **B3** and **B4** (left), and crystal data and structure refinement (right). Thermal ellipsoids are shown at 50% probability; hydrogen atoms have been omitted for clarity.

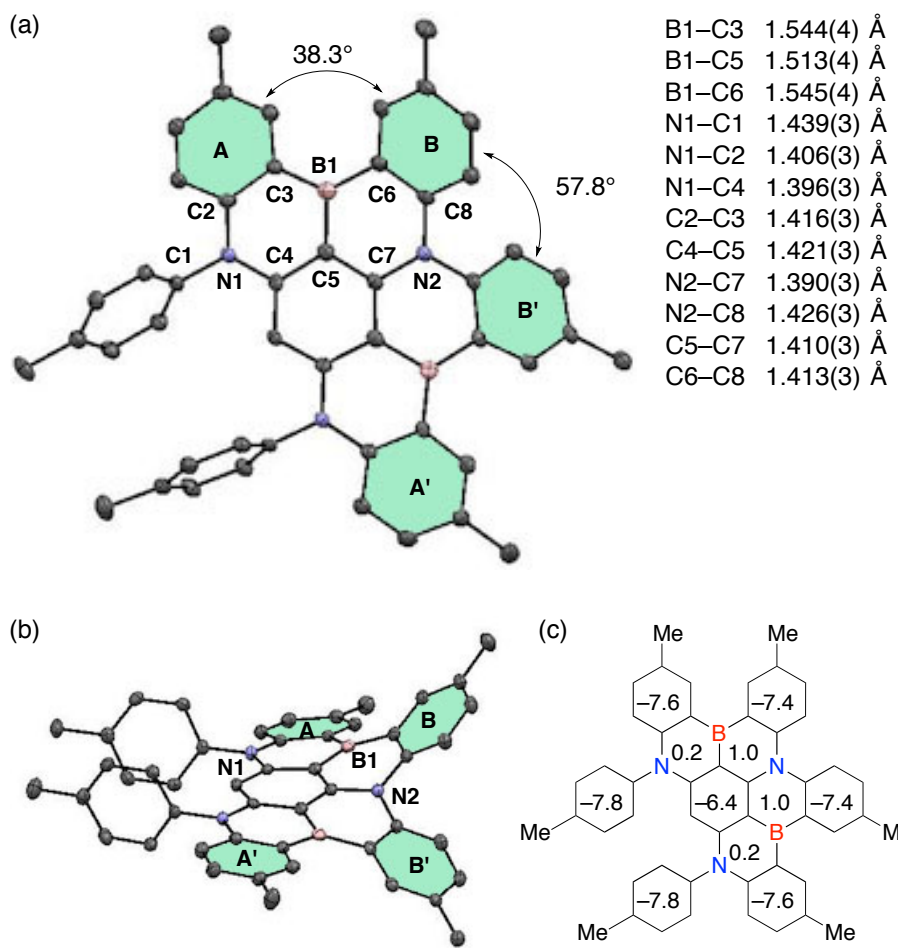


Figure S3. (a and b) ORTEP drawings of **B2** obtained by X-ray crystallographic analysis. Thermal ellipsoids are shown at 50% probability. Hydrogen atoms are omitted for clarity. (c) NICS(0) values for **B2** calculated at the B3LYP/6-311+G(d,p) level of theory.

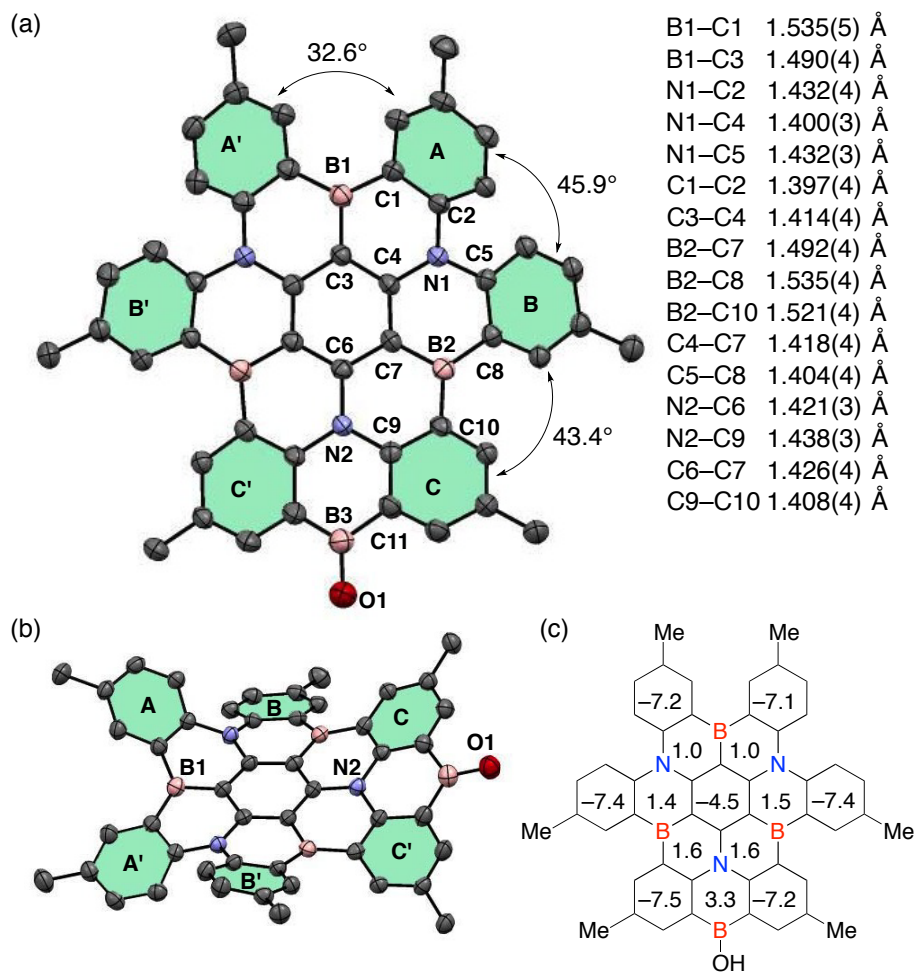


Figure S4. (a and b) ORTEP drawings of **B4** obtained by X-ray crystallographic analysis. Thermal ellipsoids are shown at 50% probability. Hydrogen atoms are omitted for clarity. (c) NICS(0) values for **B4** calculated at the B3LYP/6-311+G(d,p) level of theory.

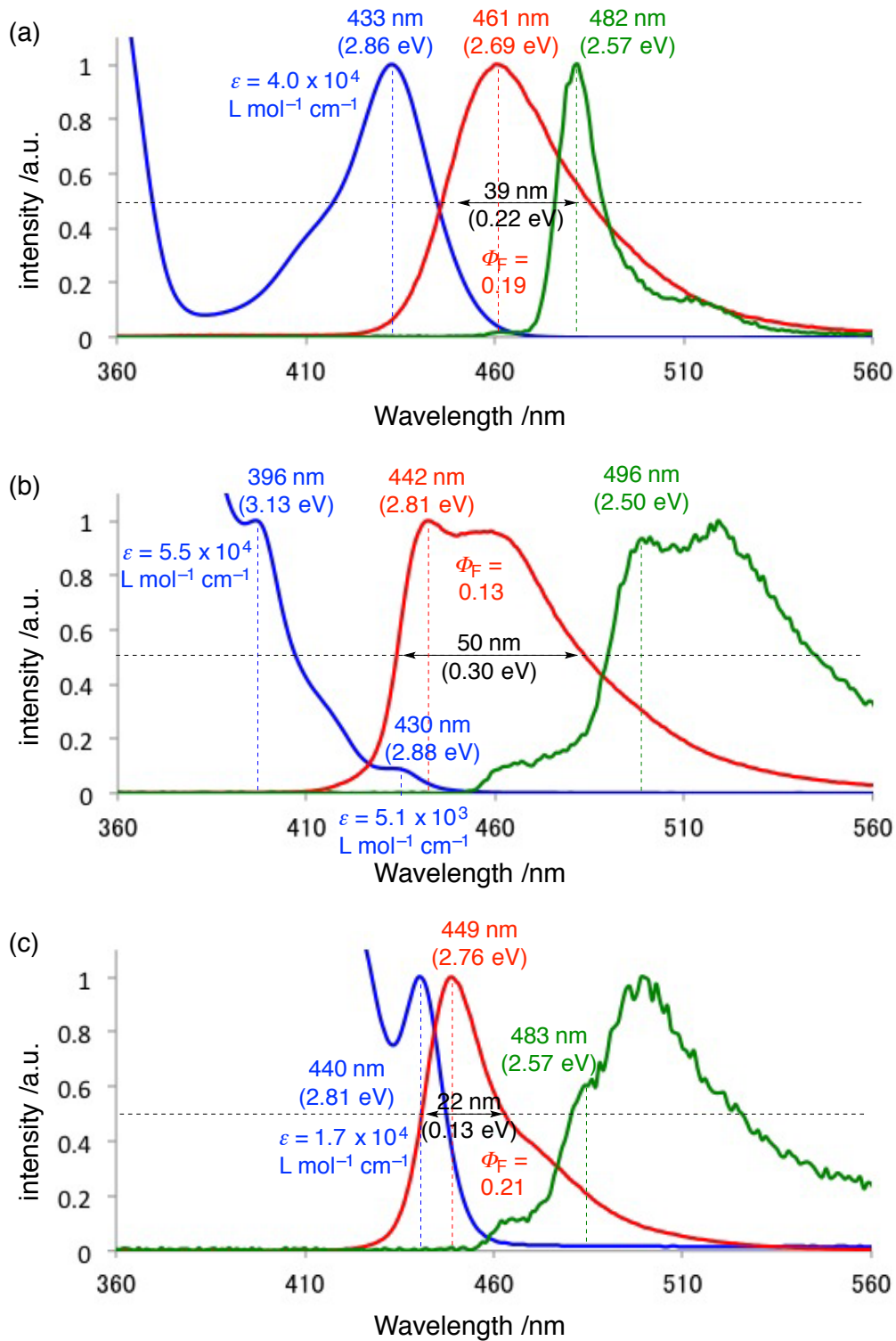


Figure S5. Normalized absorption (blue, 0.02 mM in CH_2Cl_2), fluorescence (red, 0.02 mM in CH_2Cl_2) and phosphorescence (green, 77 K, saturated in 2-methyltetrahydrofuran, 100–200 μsec delay) spectra with absorption/emission maxima (nm, eV), absorption coefficient at an absorption maximum (ε), absolute fluorescence quantum yield (Φ_F), and full width at half maximum (nm, eV) of (a) **B2**, (b) **B3** and (c) **B4** (excited at 340 nm).

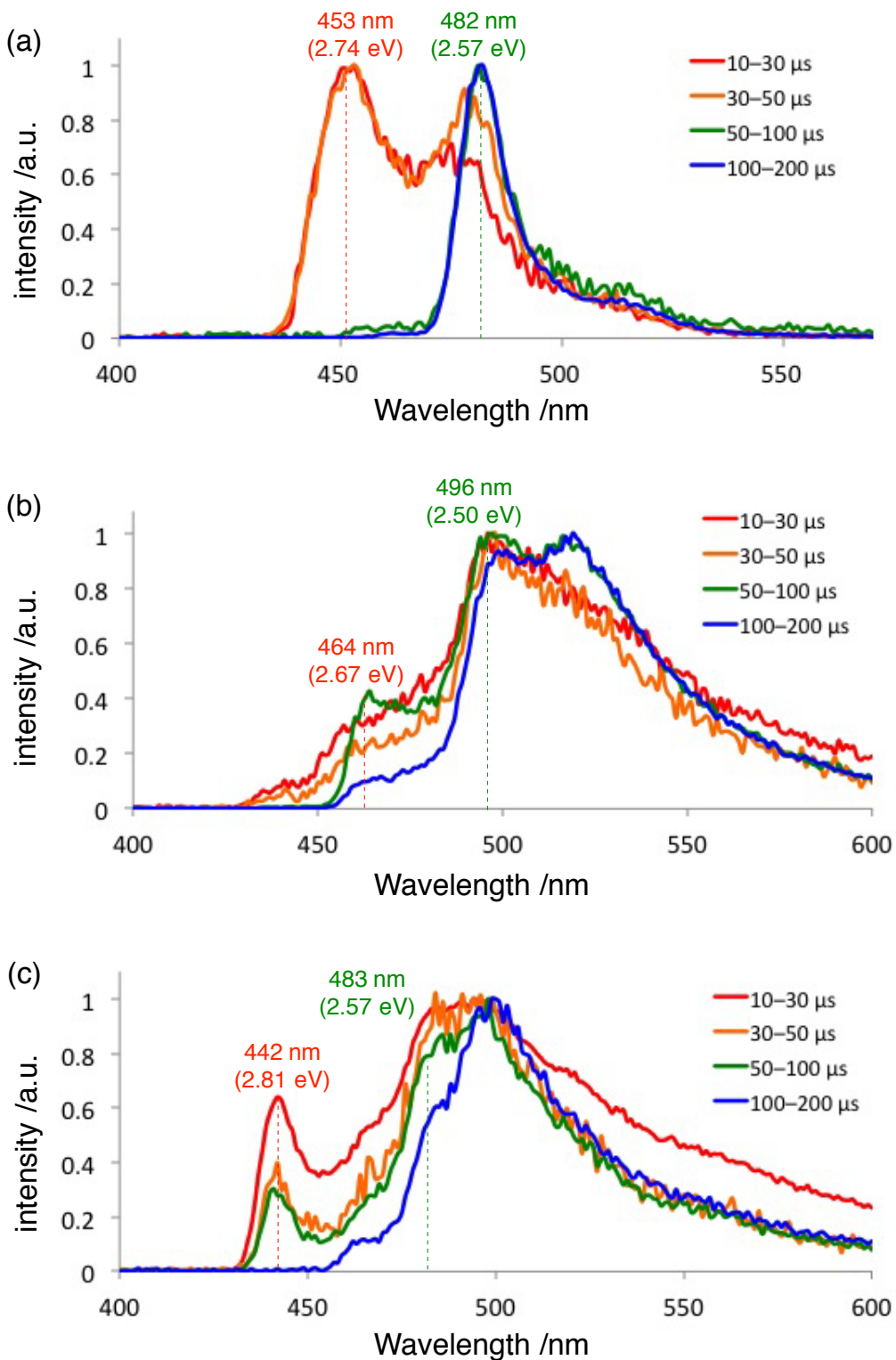


Figure S6. Photoluminescence (PL) spectra. Normalized PL spectra of compounds (a) **B2**, (b) **B3** and (c) **B4** at 77 K with various delay times (saturated in 2-methyltetrahydrofuran).

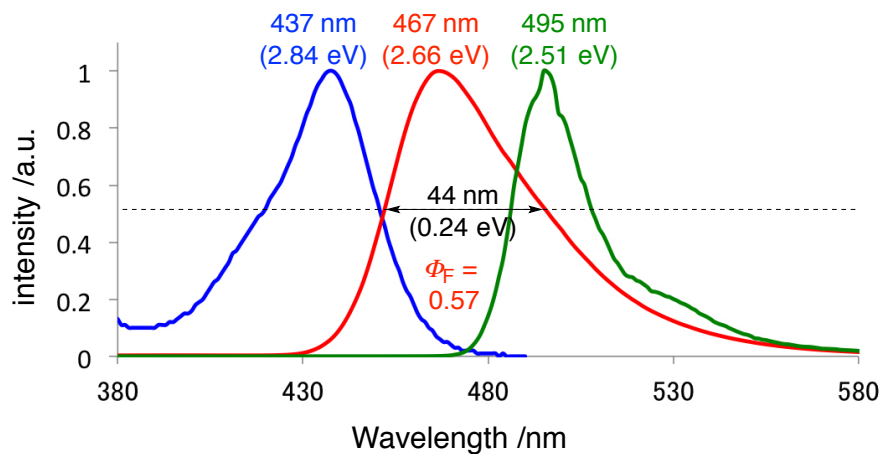


Figure S7. Normalized absorption (blue), fluorescence (red), and phosphorescence (green, 77 K) spectra with absorption/emission maxima (nm, eV), absolute fluorescence quantum yield (Φ_F), and full width at half maximum (nm, eV) of a PMMA film of **B2-F** (1 wt.%, excited at 360 nm).

Measurement of differential pulse voltammograms. Differential pulse voltammetry was conducted on a BAS Electrochemical Analyzer ALS 604E and CS-3A using a three-electrode cell with a glassy carbon working electrode, a platinum wire counter electrode, and an Ag/AgNO₃ reference electrode.

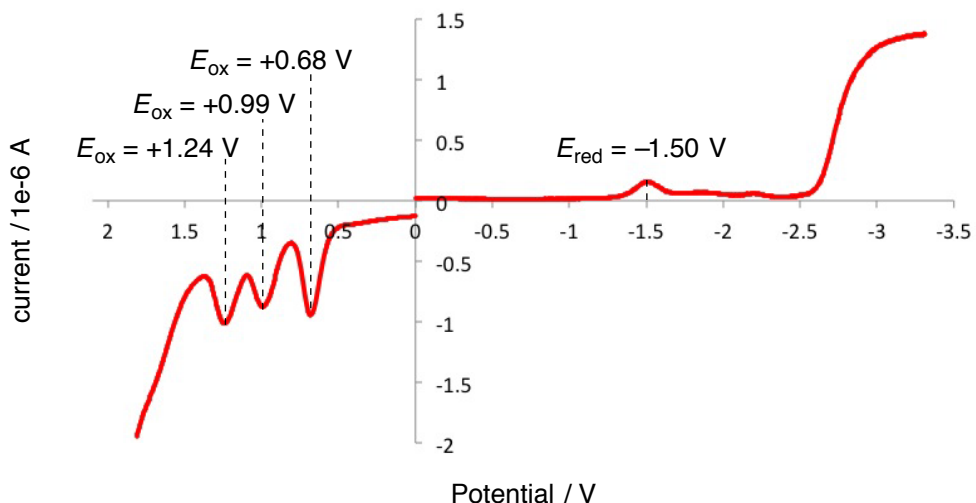


Figure S8. Differential pulse voltammograms of **B3** saturated in 1,2-dichlorobenzene with 0.08 M *n*-Bu₄N⁺PF₆⁻. Oxidation (E_{ox}) and reduction (E_{red}) potentials are given in V versus the ferrocene/ferrocenium couple.

Estimation of rate constant for reverse intersystem crossing. Rate constants (k_F , k_{IC} , k_{ISC} , and k_{RISC}) were determined from the measurements of quantum yields (Φ_F and Φ_{TADF}) and lifetimes (τ_F , τ_{TADF}) and of the prompt (fluorescence) and delayed (TADF) components according to Adachi's method (equations 1–2¹², 3–5¹³ and 6¹⁴).

$$\Phi = 0.676$$

$$\Phi_F = 0.201$$

$$\Phi_{TADF} = 0.475$$

$$\tau_F = 2.81 \text{ ns}$$

$$\tau_{TADF} = 82.9 \mu\text{s}$$

$$k_p = 3.6 \times 10^8 \text{ s}^{-1} \quad k_p = 1/\tau_F \quad (1)$$

$$k_d = 1.2 \times 10^4 \text{ s}^{-1} \quad k_d = 1/\tau_{TADF} \quad (2)$$

$$k_F = 7.1 \times 10^7 \text{ s}^{-1} \quad k_F = \Phi_F/\tau_F \quad (3)$$

$$k_{IC} = 3.4 \times 10^7 \text{ s}^{-1} \quad \Phi = k_F/(k_F + k_{IC}) \quad (4)$$

$$k_{ISC} = 2.5 \times 10^8 \text{ s}^{-1} \quad \Phi_F = k_F/(k_F + k_{IC} + k_{ISC}) \quad (5)$$

$$k_{RISC} = 4.1 \times 10^4 \text{ s}^{-1} \quad k_{RISC} = k_p k_d / (k_p - k_{ISC}) \quad (6)$$

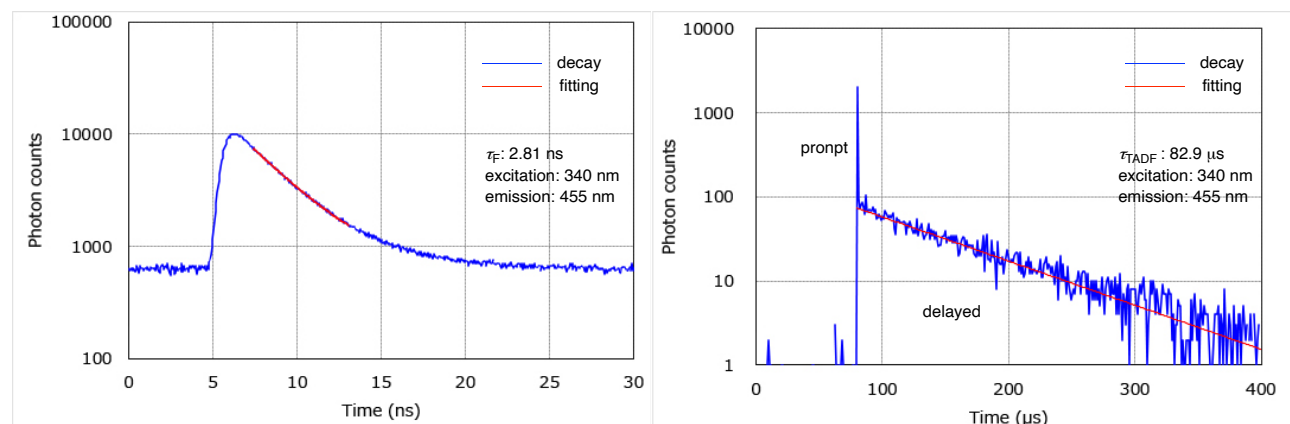


Figure S9. Transient decay spectra of a PMMA film (1 wt%, dispersed) of **B2** at 300 K. A red curve is single exponential fitting data.

Device fabrication and measurement of electroluminescence characteristics. OLED was fabricated on glass substrates coated with a patterned transparent ITO conductive layer. Substrates were cleaned in a detergent solution for 5 min, sonicated in distilled water for 10 min, and pre-dried with a jet spin washer, followed by 5-min drying in an oven at 150 °C and treatment with UV ozone. OLED employing **B2** as an emitter with the following structure was fabricated: indium tin oxide (ITO, 50 nm); *N,N'*-di(1-naphthyl)-*N,N'*-diphenyl-(1,1'-biphenyl)-4,4'-diamine (NPD, 40 nm); tris(4-carbazolyl-9-ylphenyl)amine (TCTA, 15 nm); 1,3-bis(*N*-carbazolyl)benzene (mCP, 15 nm); 1 wt% **B2** and 99 wt% of mCBP (20 nm); diphenyl-4-triphenylsilylphenylphosphine oxide (TSPO1, 40 nm); LiF (1 nm); Al (100 nm). During deposition, the vacuum evaporation pressure equaled 5.0×10^{-4} Pa, and the film thickness was controlled with a calibrated quartz crystal microbalance. After the deposition of all layers, the fabricated OLED test modules were placed in an evaporation chamber filled with nitrogen and covered with a capping glass. The characteristics of all fabricated devices were evaluated under ambient atmosphere at room temperature using a voltage-current-luminance measuring system, which consisted of a source meter (Keithley 2400) and a spectral radiance meter (Topcon SR-3AR). Assuming a perfectly diffusing light-emitting surface, the external quantum efficiency was calculated based on the electroluminescence (EL) spectrum.

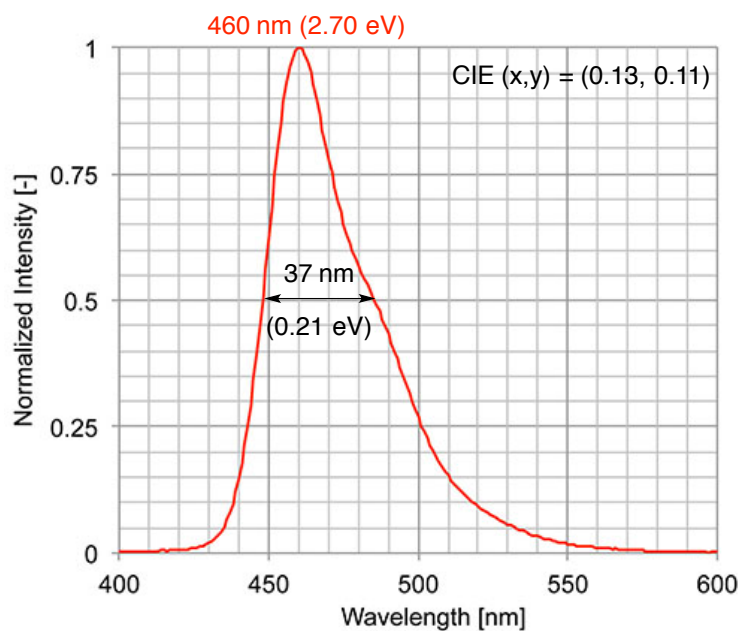


Figure S10. Electroluminescence spectrum of OLED employing **B2** as an emitter.

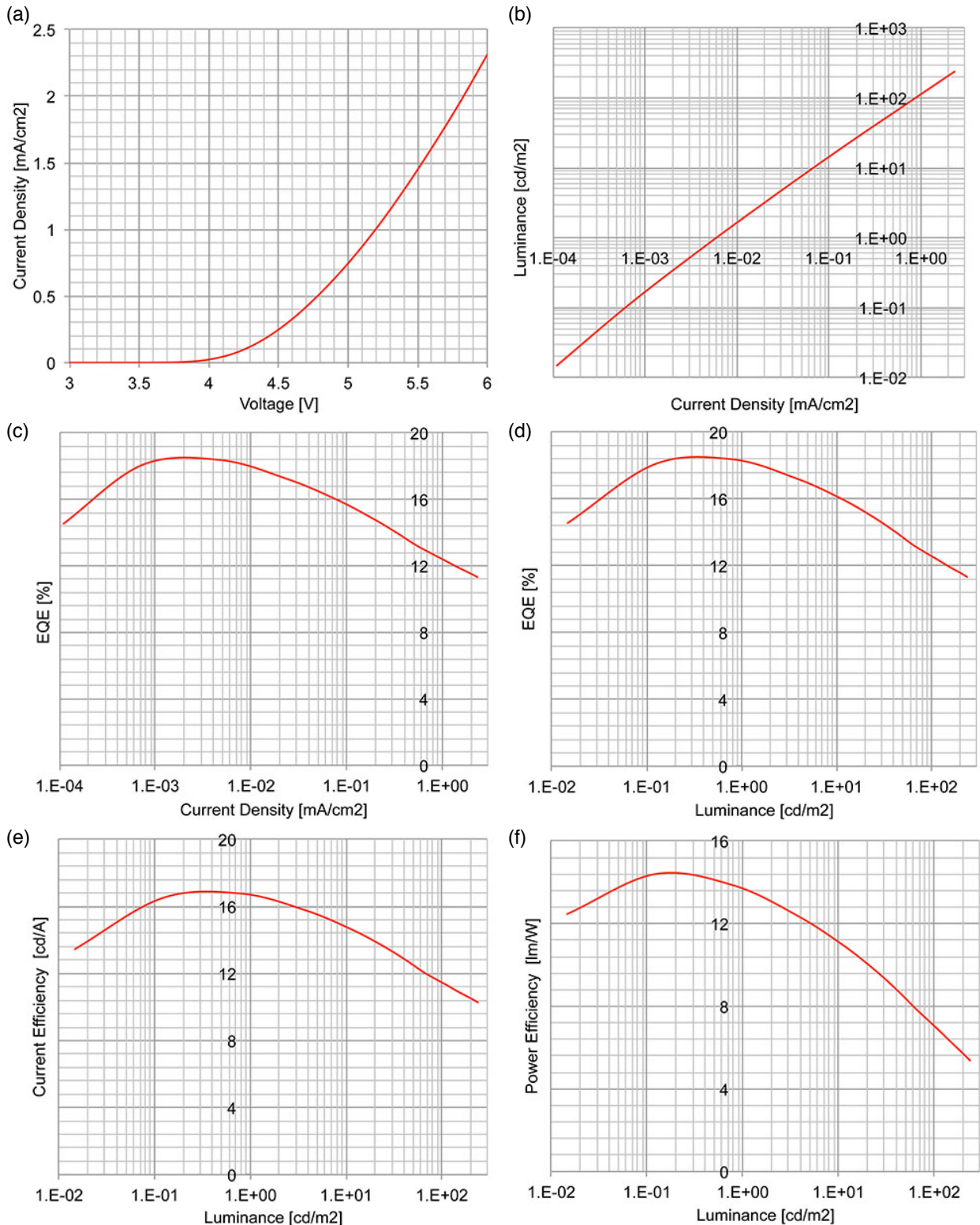


Figure S11. Characteristics of OLED device using **B2** as an emitter. (a) current density vs. driving voltage, (b) luminance vs. current density, (c) external quantum efficiency (EQE) vs. current density, (d) external quantum efficiency (EQE) vs. luminance, (e) current efficiency (η_c) vs. luminance, and (f) power efficiency (η_p) vs. luminance.

Cartesian coordinates

1 (S_0 , C_3 symmetry)

E(B3LYP/6-31G(d)) = -2020.49930815 hartree

E(B3LYP/6-311+G(d,p)) = -2020.99429030 hartree (TD-DFT)

Center Number	Atomic Number	Atomic Type	Coordinates (Angstroms)		
			X	Y	Z
1	7	0	0.000000	2.823467	0.000009
2	7	0	2.445194	-1.411733	0.000009
3	7	0	-2.445194	-1.411733	0.000009
4	6	0	-1.214271	-0.700841	-0.000375
5	6	0	-0.000208	-1.401039	-0.000469
6	6	0	1.214082	-0.701169	-0.000375
7	6	0	1.213439	0.700339	-0.000469
8	6	0	0.000189	1.402010	-0.000375
9	6	0	-1.213231	0.700700	-0.000469
10	1	0	-0.000714	-2.484189	-0.001028
11	1	0	2.151728	1.241476	-0.001028
12	1	0	-2.151014	1.242713	-0.001028
13	6	0	-0.937003	3.535895	0.797603
14	6	0	-1.597193	4.666282	0.292603
15	6	0	-1.215902	3.131138	2.112022
16	6	0	-2.500958	5.368888	1.085924
17	1	0	-1.394150	4.994008	-0.722104
18	6	0	-2.136579	3.832237	2.886558
19	1	0	-0.704904	2.266075	2.522887
20	6	0	-2.797880	4.965089	2.394144
21	1	0	-2.996240	6.244344	0.671008
22	1	0	-2.332706	3.498729	3.903546
23	6	0	0.936160	3.537004	-0.797368
24	6	0	1.590002	4.672287	-0.295246
25	6	0	1.221005	3.128195	-2.109534
26	6	0	2.493980	5.374961	-1.088573
27	1	0	1.382482	5.004084	0.717223
28	6	0	2.141399	3.829568	-2.883817

29	1	0	0.715288	2.259227	-2.518676
30	6	0	2.797177	4.966846	-2.393807
31	1	0	2.984529	6.253941	-0.675524
32	1	0	2.342105	3.492510	-3.898765
33	6	0	-3.811914	5.706996	3.233007
34	1	0	-3.843528	6.771594	2.976574
35	1	0	-4.825026	5.308295	3.085422
36	1	0	-3.585401	5.624677	4.301744
37	6	0	3.812333	5.707290	-3.232545
38	1	0	4.820570	5.289827	-3.104884
39	1	0	3.571532	5.647194	-4.299741
40	1	0	3.864223	6.766640	-2.958515
41	6	0	-2.593673	-2.579416	0.797603
42	6	0	-2.103694	-2.618571	2.112022
43	6	0	-3.242522	-3.716351	0.292603
44	6	0	-2.250525	-3.766450	2.886558
45	1	0	-1.610026	-1.743502	2.522887
46	6	0	-3.399114	-4.850337	1.085924
47	1	0	-3.627863	-3.704373	-0.722104
48	6	0	-2.900953	-4.905580	2.394144
49	1	0	-1.863635	-3.769547	3.903546
50	1	0	-3.909641	-5.716992	0.671008
51	6	0	2.595055	-2.579240	-0.797368
52	6	0	2.098594	-2.621519	-2.109534
53	6	0	3.251318	-3.713126	-0.295246
54	6	0	2.245804	-3.769290	-2.883817
55	1	0	1.598904	-1.749071	-2.518676
56	6	0	3.407863	-4.847331	-1.088573
57	1	0	3.642423	-3.699307	0.717223
58	6	0	2.902826	-4.905849	-2.393807
59	1	0	1.853550	-3.774577	-3.898765
60	1	0	3.923807	-5.711648	-0.675524
61	6	0	3.530676	-0.956479	0.797603
62	6	0	4.839715	-0.949931	0.292603
63	6	0	3.319596	-0.512567	2.112022
64	6	0	5.900072	-0.518551	1.085924

65	1	0	5.022013	-1.289635	-0.722104
66	6	0	4.387104	-0.065787	2.886558
67	1	0	2.314930	-0.522573	2.522887
68	6	0	5.698833	-0.059509	2.394144
69	1	0	6.905881	-0.527352	0.671008
70	1	0	4.196341	0.270818	3.903546
71	6	0	-3.531215	-0.957764	-0.797368
72	6	0	-4.841320	-0.959161	-0.295246
73	6	0	-3.319599	-0.506676	-2.109534
74	6	0	-5.901843	-0.527630	-1.088573
75	1	0	-5.024905	-1.304777	0.717223
76	6	0	-4.387203	-0.060278	-2.883817
77	1	0	-2.314192	-0.510156	-2.518676
78	6	0	-5.700003	-0.060997	-2.393807
79	1	0	-6.908336	-0.542293	-0.675524
80	1	0	-4.195655	0.282067	-3.898765
81	6	0	-3.036446	-6.154712	3.233007
82	1	0	-3.078413	-5.917387	4.301744
83	1	0	-3.942608	-6.714390	2.976574
84	1	0	-2.184605	-6.832743	3.085422
85	6	0	-6.848825	0.447932	-3.232545
86	1	0	-6.991410	1.529823	-3.104884
87	1	0	-6.676379	0.269440	-4.299741
88	1	0	-7.792194	-0.036805	-2.958515
89	6	0	3.036492	-6.155222	-3.232545
90	1	0	3.927971	-6.729835	-2.958515
91	1	0	2.170840	-6.819650	-3.104884
92	1	0	3.104847	-5.916634	-4.299741
93	6	0	6.848360	0.447716	3.233007
94	1	0	7.009631	1.524448	3.085422
95	1	0	6.663814	0.292710	4.301744
96	1	0	7.786136	-0.057204	2.976574

B2 (S₀, C₂ symmetry)

E(B3LYP/6-31G(d)) = -2066.72711935 hartree

$E(B3LYP/6-311+G(d,p)) = -2067.20852932$ hartree (TD-DFT)

Center Number	Atomic Number	Atomic Type	Coordinates (Angstroms)		
			X	Y	Z
1	5	0	0.366127	2.522063	1.522062
2	5	0	-0.366127	-2.522063	1.522062
3	7	0	0.000000	0.000000	2.856136
4	7	0	0.163307	2.421354	-1.347517
5	7	0	-0.163307	-2.421354	-1.347517
6	6	0	-0.099170	-1.208309	-0.650811
7	6	0	0.000000	0.000000	-1.355678
8	6	0	0.099170	1.208309	-0.650811
9	6	0	0.154113	1.230782	0.771062
10	6	0	0.000000	0.000000	1.452240
11	6	0	-0.154113	-1.230782	0.771062
12	1	0	0.000000	0.000000	-2.433832
13	6	0	-0.664585	-1.042734	3.564686
14	6	0	-0.815785	-2.329581	2.990752
15	6	0	-1.259790	-0.759933	4.810141
16	6	0	-1.537579	-3.291314	3.732765
17	6	0	-1.947609	-1.742855	5.503261
18	1	0	-1.208079	0.241477	5.220982
19	6	0	-2.093014	-3.040379	4.982730
20	1	0	-1.703015	-4.266052	3.283489
21	1	0	-2.409188	-1.489684	6.455731
22	6	0	0.664585	1.042734	3.564686
23	6	0	0.815785	2.329581	2.990752
24	6	0	1.259790	0.759933	4.810141
25	6	0	1.537579	3.291314	3.732765
26	6	0	1.947609	1.742855	5.503261
27	1	0	1.208079	-0.241477	5.220982
28	6	0	2.093014	3.040379	4.982730
29	1	0	1.703015	4.266052	3.283489
30	1	0	2.409188	1.489684	6.455731
31	6	0	0.148404	3.687963	-0.721660

32	6	0	0.221680	3.811912	0.691878
33	6	0	0.052262	4.852392	-1.515202
34	6	0	0.120783	5.110448	1.238863
35	6	0	-0.014972	6.103590	-0.923722
36	1	0	0.014628	4.780491	-2.594752
37	6	0	0.000000	6.263701	0.472576
38	1	0	0.115770	5.207776	2.321021
39	1	0	-0.097505	6.980050	-1.563951
40	6	0	0.184195	2.380530	-2.788188
41	6	0	-1.009191	2.357399	-3.512906
42	6	0	1.404642	2.380849	-3.467600
43	6	0	-0.977200	2.336838	-4.907172
44	1	0	-1.955469	2.362319	-2.980182
45	6	0	1.426092	2.361454	-4.861282
46	1	0	2.329494	2.404584	-2.898834
47	6	0	0.237887	2.337090	-5.604453
48	1	0	-1.912555	2.324556	-5.461824
49	1	0	2.381988	2.368230	-5.380145
50	6	0	-0.184195	-2.380530	-2.788188
51	6	0	1.009191	-2.357399	-3.512906
52	6	0	-1.404642	-2.380849	-3.467600
53	6	0	0.977200	-2.336838	-4.907172
54	1	0	1.955469	-2.362319	-2.980182
55	6	0	-1.426092	-2.361454	-4.861282
56	1	0	-2.329494	-2.404584	-2.898834
57	6	0	-0.237887	-2.337090	-5.604453
58	1	0	1.912555	-2.324556	-5.461824
59	1	0	-2.381988	-2.368230	-5.380145
60	6	0	-0.148404	-3.687963	-0.721660
61	6	0	-0.221680	-3.811912	0.691878
62	6	0	-0.052262	-4.852392	-1.515202
63	6	0	-0.120783	-5.110448	1.238863
64	6	0	0.014972	-6.103590	-0.923722
65	1	0	-0.014628	-4.780491	-2.594752
66	6	0	0.000000	-6.263701	0.472576
67	1	0	-0.115770	-5.207776	2.321021

68	1	0	0.097505	-6.980050	-1.563951
69	6	0	2.845383	4.103150	5.747994
70	1	0	3.030416	4.985234	5.126564
71	1	0	2.285147	4.434474	6.632625
72	1	0	3.814972	3.733657	6.104038
73	6	0	-0.111988	7.633268	1.099926
74	1	0	-0.095961	7.571480	2.192854
75	1	0	0.713772	8.288027	0.792170
76	1	0	-1.043315	8.136343	0.809413
77	6	0	0.269678	2.289724	-7.114381
78	1	0	-0.662664	2.666262	-7.547464
79	1	0	1.095512	2.885752	-7.517850
80	1	0	0.407186	1.261747	-7.476373
81	6	0	-0.269678	-2.289724	-7.114381
82	1	0	-0.407186	-1.261747	-7.476373
83	1	0	0.662664	-2.666262	-7.547464
84	1	0	-1.095512	-2.885752	-7.517850
85	6	0	0.111988	-7.633268	1.099926
86	1	0	-0.713772	-8.288027	0.792170
87	1	0	1.043315	-8.136343	0.809413
88	1	0	0.095961	-7.571480	2.192854
89	6	0	-2.845383	-4.103150	5.747994
90	1	0	-2.285147	-4.434474	6.632625
91	1	0	-3.814972	-3.733657	6.104038
92	1	0	-3.030416	-4.985234	5.126564

B3 (S_0 , C_3 symmetry)

E(B3LYP/6-31G(d)) = -2089.82745452 hartree

E(B3LYP/6-311+G(d,p)) = -2090.30147741 hartree (TD-DFT)

E(B3LYP/6-311+G(d,p)) = -2090.30144868 hartree (NICS)

Center Number	Atomic Number	Atomic Type	Coordinates (Angstroms)		
			X	Y	Z
1	5	0	-0.989913	2.768235	-0.001488
			S30		

2	5	0	2.892318	-0.526829	-0.001488
3	5	0	-1.902405	-2.241408	-0.001488
4	7	0	1.812914	2.136108	-0.004016
5	7	0	0.943466	-2.638083	-0.004016
6	7	0	-2.756381	0.501976	-0.004016
7	6	0	-0.482217	1.348390	-0.004387
8	6	0	0.906548	1.068087	-0.004461
9	6	0	1.408849	-0.256582	-0.004387
10	6	0	0.471717	-1.319138	-0.004461
11	6	0	-0.926632	-1.091808	-0.004387
12	6	0	-1.378265	0.251050	-0.004461
13	6	0	-2.458844	2.919518	0.438437
14	6	0	-3.004349	4.108752	0.969657
15	6	0	-3.254352	1.747794	0.487508
16	6	0	-4.268934	4.180184	1.543628
17	1	0	-2.384617	5.001854	0.963127
18	6	0	-4.517373	1.794683	1.108702
19	6	0	-5.009724	2.987378	1.615712
20	1	0	-5.103352	0.890180	1.220089
21	1	0	-5.982530	2.987848	2.103327
22	6	0	1.407263	3.415945	-0.492862
23	6	0	2.353178	4.253388	-1.115115
24	6	0	0.049714	3.818393	-0.438815
25	6	0	1.977498	5.489880	-1.616978
26	1	0	3.379011	3.924189	-1.230413
27	6	0	-0.282615	5.086384	-0.963863
28	6	0	0.649245	5.944192	-1.537978
29	1	0	2.728404	6.107791	-2.105307
30	1	0	-1.327588	5.385803	-0.952259
31	6	0	3.757799	0.669663	0.438437
32	6	0	3.140810	1.944455	0.487508
33	6	0	5.060458	0.547466	0.969657
34	6	0	3.812927	3.014817	1.108702
35	6	0	5.754613	1.606913	1.543628
36	1	0	5.524040	-0.435787	0.963127
37	6	0	5.092007	2.844859	1.615712

38	1	0	3.322595	3.974543	1.220089
39	1	0	5.578817	3.687099	2.103327
40	6	0	2.254663	-2.926698	-0.492862
41	6	0	3.281969	-1.952251	-0.438815
42	6	0	2.506952	-4.164605	-1.115115
43	6	0	4.546246	-2.298440	-0.963863
44	6	0	3.765627	-4.457504	-1.616978
45	1	0	1.708942	-4.888404	-1.230413
46	6	0	4.823199	-3.534358	-1.537978
47	1	0	5.328036	-1.543177	-0.952259
48	1	0	3.925300	-5.416763	-2.105307
49	6	0	-1.298955	-3.589180	0.438437
50	6	0	0.113543	-3.692248	0.487508
51	6	0	-2.056109	-4.656218	0.969657
52	6	0	0.704445	-4.809500	1.108702
53	6	0	-1.485679	-5.787097	1.543628
54	1	0	-3.139424	-4.566065	0.963127
55	6	0	-0.082283	-5.832237	1.615712
56	1	0	1.780758	-4.864723	1.220089
57	1	0	0.403712	-6.674947	2.103327
58	6	0	-3.331683	-1.866144	-0.438815
59	6	0	-3.661926	-0.489246	-0.492862
60	6	0	-4.263630	-2.787944	-0.963863
61	6	0	-4.860131	-0.088781	-1.115115
62	6	0	-5.472444	-2.409833	-1.537978
63	1	0	-4.000448	-3.842626	-0.952259
64	6	0	-5.743125	-1.032377	-1.616978
65	1	0	-5.087953	0.964215	-1.230413
66	1	0	-6.653705	-0.691029	-2.105307
67	6	0	6.190186	-3.873001	-2.083216
68	1	0	6.852471	-3.001636	-2.066249
69	1	0	6.671520	-4.666426	-1.496404
70	1	0	6.133354	-4.231034	-3.118635
71	6	0	0.259024	7.297360	-2.083216
72	1	0	-0.826743	7.435233	-2.066249
73	1	0	0.705485	8.110919	-1.496404

74	1	0	0.597507	7.427157	-3.118635
75	6	0	-6.449211	-3.424358	-2.083216
76	1	0	-6.025729	-4.433597	-2.066249
77	1	0	-7.377004	-3.444492	-1.496404
78	1	0	-6.730860	-3.196123	-3.118635
79	6	0	-2.327082	-6.913869	2.094153
80	1	0	-3.389716	-6.651119	2.099945
81	1	0	-2.215443	-7.827833	1.495910
82	1	0	-2.038376	-7.167145	3.121689
83	6	0	-4.824045	5.472247	2.094153
84	1	0	-4.065180	6.261139	2.099945
85	1	0	-5.671380	5.832546	1.495910
86	1	0	-5.187741	5.348859	3.121689
87	6	0	7.151127	1.441622	2.094153
88	1	0	7.454896	0.389979	2.099945
89	1	0	7.886823	1.995286	1.495910
90	1	0	7.226117	1.818287	3.121689

B4 (S_0 , C_1 symmetry)

E(B3LYP/6-31G(d)) = -2189.38364185 hartree

E(B3LYP/6-311+G(d,p)) = -2189.78485926 hartree (TD-DFT)

E(B3LYP/6-311+G(d,p)) = -2189.88927111 hartree (NICS)

Center Number	Atomic Number	Atomic Type	Coordinates (Angstroms)		
			X	Y	Z
1	5	-0.000059930	0.000008039	0.000049453	
2	5	-0.000023776	-0.000057538	0.000000830	
3	5	-0.000035110	-0.000017261	0.000022740	
4	5	-0.000083053	-0.000007072	0.000015753	
5	7	0.000080350	0.000049097	-0.000004741	
6	7	0.000050263	-0.000059818	0.000003315	
7	7	0.000018852	-0.000001278	-0.000063107	
8	6	-0.000008621	-0.000006579	0.000030112	
9	6	0.000037799	-0.000000492	-0.000041736	

10	6	-0.000037064	0.000018472	0.000001260
11	6	0.000061688	0.000033526	-0.000052755
12	6	-0.000078753	-0.000012539	0.000060706
13	6	0.000029366	0.000020599	-0.000036693
14	6	-0.000069977	-0.000038812	-0.000007126
15	6	0.000022721	0.000053313	0.000017243
16	6	0.000005119	0.000029047	-0.000004106
17	6	0.000008401	-0.000004290	-0.000069602
18	6	0.000012733	-0.000009919	0.000017289
19	1	0.000033941	0.000009951	0.000000699
20	6	-0.000005051	0.000015630	-0.000018595
21	1	0.000078811	-0.000089681	-0.000023281
22	1	0.000000936	-0.000011390	0.000003654
23	6	-0.000016560	-0.000028745	-0.000033029
24	6	0.000051367	0.000037509	-0.000020672
25	6	-0.000031544	-0.000005662	0.000001830
26	6	0.000002207	-0.000029980	0.000028200
27	6	-0.000010493	0.000014463	0.000016745
28	1	-0.000015514	-0.000011490	-0.000000016
29	6	-0.000026595	0.000005543	-0.000006654
30	1	-0.000007839	0.000017550	-0.000024999
31	1	-0.000000751	0.000000753	0.000001744
32	6	-0.000031370	-0.000001834	0.000008198
33	6	0.000002413	-0.000013955	-0.000035517
34	6	-0.000038310	0.000032540	0.000005698
35	6	0.000002765	-0.000005197	-0.000006237
36	6	-0.000006179	-0.000005006	-0.000003378
37	1	-0.000009986	0.000026437	0.000025590
38	6	0.000004915	-0.000030601	0.000034895
39	1	0.000039503	0.000002136	0.000015313
40	1	0.000010277	0.000005421	-0.000001817
41	6	-0.000015551	-0.000004872	-0.000032051
42	6	0.000020544	-0.000008209	0.000027933
43	6	0.000035986	-0.000022993	-0.000002256
44	6	0.000010926	0.000003513	-0.000004713
45	6	-0.000013456	0.000008122	-0.000005485

46	1	0.000013286	-0.000010747	0.000000916
47	6	0.000001229	0.000010364	-0.000010058
48	1	0.000022569	0.000007801	0.000008595
49	1	0.000001282	0.000000892	0.000002879
50	6	-0.000004831	0.000006367	0.000007312
51	6	0.000008264	0.000007928	0.000012049
52	6	-0.000003579	0.000060805	-0.000017189
53	6	0.000014416	-0.000018853	0.000003325
54	6	-0.000007657	-0.000045873	0.000012508
55	6	0.000017617	0.000040806	0.000003481
56	1	0.000002992	0.000011858	-0.000011499
57	1	-0.000024472	-0.000012298	-0.000001278
58	6	-0.000044057	0.000018710	0.000009369
59	6	-0.000014234	-0.000015418	0.000029525
60	6	0.000084645	-0.000024714	-0.000026319
61	6	-0.000017821	0.000031063	0.000005445
62	6	0.000013058	-0.000000413	0.000009451
63	6	0.000002370	0.000010970	-0.000000281
64	1	-0.000083178	0.000026082	0.000070707
65	1	0.000002140	-0.000001901	0.000004366
66	6	0.000010463	0.000004564	-0.000001375
67	1	-0.000011411	-0.000002337	0.000004206
68	1	0.000002336	-0.000017765	0.000003736
69	1	0.000010955	0.000005734	-0.000007480
70	6	-0.000003406	0.000018120	-0.000002271
71	1	0.000007056	0.000000710	-0.000004595
72	1	-0.000003162	0.000004534	0.000004814
73	1	-0.000001742	-0.000011662	-0.000007078
74	6	0.000001209	-0.000010926	-0.000008426
75	1	-0.000008355	0.000002050	0.000000498
76	1	0.000008367	0.000005548	0.000009679
77	1	0.000005547	-0.000007691	-0.000002126
78	6	-0.000012868	-0.000009233	0.000001017
79	1	0.000001368	-0.000003606	-0.000007506
80	1	0.000001931	-0.000004196	0.000007182
81	1	0.000003805	0.000007113	-0.000004102

82	6	0.000008171	0.000009438	-0.000003767
83	1	-0.000004956	-0.000002346	-0.000000272
84	1	-0.000002005	0.000000074	-0.000000287
85	1	-0.000002336	-0.000001121	0.000001716
86	6	0.000006073	-0.000002833	0.000009955
87	1	-0.000009967	0.000005856	0.000003390
88	1	-0.000011386	0.000003179	-0.000012052
89	1	0.000007460	-0.000002397	0.000003754
90	8	0.000028530	0.000010239	-0.000003534
91	1	-0.000012114	-0.000010921	0.000010984

2,7,10,15,18,23-hexamethylhexabenz[a,d,g,j,m,p]coronene (S_0 , C_3 symmetry)

E(B3LYP/6-31G(d)) = -2079.60986132 hartree

E(B3LYP/6-311+G(d,p)) = -2080.07206209 hartree (NICS)

Center Number	Atomic Number	Atomic Type	Coordinates (Angstroms)		
			X	Y	Z
1	6	0	-1.441154	0.000002	-0.000145
2	6	0	-0.720058	1.247177	-0.000233
3	6	0	0.720579	1.248075	-0.000145
4	6	0	1.440115	0.000000	-0.000233
5	6	0	0.720576	-1.248077	-0.000145
6	6	0	-0.720058	-1.247177	-0.000233
7	6	0	-3.526464	-1.211574	0.415142
8	6	0	-4.838046	-1.191023	0.954324
9	6	0	-2.811043	-2.447118	0.411496
10	6	0	-5.462217	-2.323137	1.451226
11	1	0	-5.350494	-0.239762	1.040456
12	6	0	-3.455469	-3.591020	0.947521
13	6	0	-4.743436	-3.537180	1.438367
14	1	0	-2.900016	-4.517018	1.034751
15	1	0	-5.192645	-4.431967	1.863759
16	6	0	-2.811126	2.446851	-0.412095
17	6	0	-3.455251	3.590327	-0.949244

18	6	0	-3.526796	1.211433	-0.414702
19	6	0	-4.743410	3.536480	-1.439599
20	1	0	-2.899345	4.515893	-1.038344
21	6	0	-4.838756	1.190899	-0.953068
22	6	0	-5.462761	2.322788	-1.450727
23	1	0	-5.192254	4.431032	-1.865913
24	1	0	-5.351724	0.239853	-1.038228
25	6	0	0.713978	3.659794	0.415142
26	6	0	-0.713745	3.657994	0.411496
27	6	0	1.387567	4.785382	0.954324
28	6	0	-1.382180	4.788034	0.947521
29	6	0	0.719213	5.891988	1.451226
30	1	0	2.467607	4.753545	1.040456
31	6	0	-0.691570	5.876526	1.438367
32	1	0	-2.461844	4.769996	1.034751
33	1	0	-1.241874	6.712946	1.863759
34	6	0	3.524599	1.211081	-0.412095
35	6	0	2.812529	2.448579	-0.414702
36	6	0	4.836940	1.197171	-0.949244
37	6	0	3.450727	3.595036	-0.953068
38	6	0	5.434387	2.339673	-1.439599
39	1	0	5.360551	0.252960	-1.038344
40	6	0	4.742974	3.569496	-1.450727
41	1	0	2.883581	4.514803	-1.038228
42	1	0	6.433513	2.281108	-1.865913
43	6	0	2.812486	-2.448220	0.415142
44	6	0	3.524788	-1.210875	0.411496
45	6	0	3.450479	-3.594359	0.954324
46	6	0	4.837649	-1.197014	0.947521
47	6	0	4.743005	-3.568850	1.451226
48	1	0	2.882887	-4.513783	1.040456
49	6	0	5.435006	-2.339346	1.438367
50	1	0	5.361860	-0.252978	1.034751
51	1	0	6.434519	-2.280979	1.863759
52	6	0	0.714267	-3.660011	-0.414702
53	6	0	-0.713472	-3.657933	-0.412095

54	6	0	1.388029	-4.785935	-0.953068
55	6	0	-1.381689	-4.787499	-0.949244
56	6	0	0.719788	-5.892284	-1.450727
57	1	0	2.468143	-4.754656	-1.038228
58	6	0	-0.690977	-5.876154	-1.439599
59	1	0	-2.461206	-4.768853	-1.038344
60	1	0	-1.241259	-6.712140	-1.865913
61	6	0	5.386147	4.804772	-2.034050
62	1	0	4.688007	5.647323	-2.057548
63	1	0	6.261451	5.112864	-1.447233
64	1	0	5.735566	4.628497	-3.059017
65	6	0	-6.854128	2.262154	-2.034050
66	1	0	-7.234729	1.236272	-2.057548
67	1	0	-7.558595	2.866143	-1.447233
68	1	0	-6.876179	2.652898	-3.059017
69	6	0	1.467981	-7.066926	-2.034050
70	1	0	2.546722	-6.883595	-2.057548
71	1	0	1.297145	-7.979007	-1.447233
72	1	0	1.140613	-7.281395	-3.059017
73	6	0	5.385865	-4.803818	2.035560
74	1	0	4.688539	-5.647088	2.056462
75	1	0	6.263181	-5.110557	1.451064
76	1	0	5.732161	-4.627964	3.061694
77	6	0	-6.853161	-2.262387	2.035560
78	1	0	-7.234791	-1.236850	2.056462
79	1	0	-7.557462	-2.868795	1.451064
80	1	0	-6.874015	-2.650215	3.061694
81	6	0	1.467296	7.066205	2.035560
82	1	0	2.546252	6.883937	2.056462
83	1	0	1.294281	7.979352	1.451064
84	1	0	1.141854	7.278180	3.061694
85	6	0	-1.422624	-2.464102	-0.000311
86	6	0	1.423528	-2.465622	0.000223
87	6	0	2.845287	0.000023	-0.000311
88	6	0	1.423528	2.465622	0.000223
89	6	0	-1.422663	2.464079	-0.000311

90	6	0	-2.847055	0.000000	0.000223
----	---	---	-----------	----------	----------

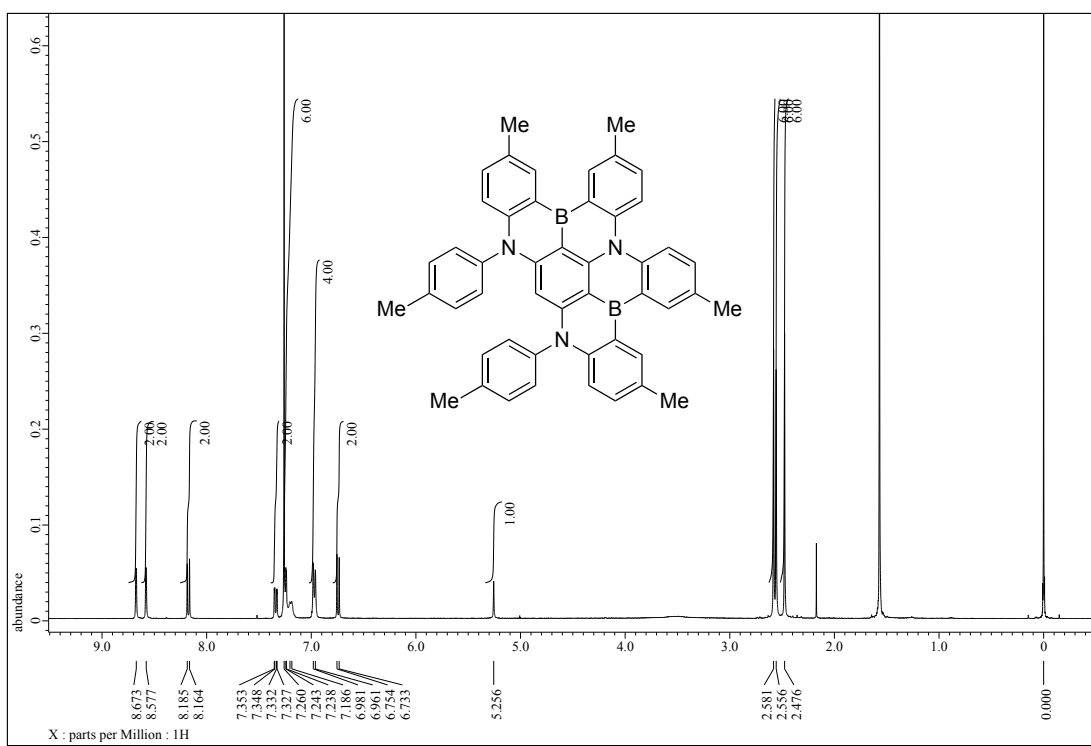


Figure S12. ^1H NMR spectrum of **B2** in CDCl_3 at 25 °C.

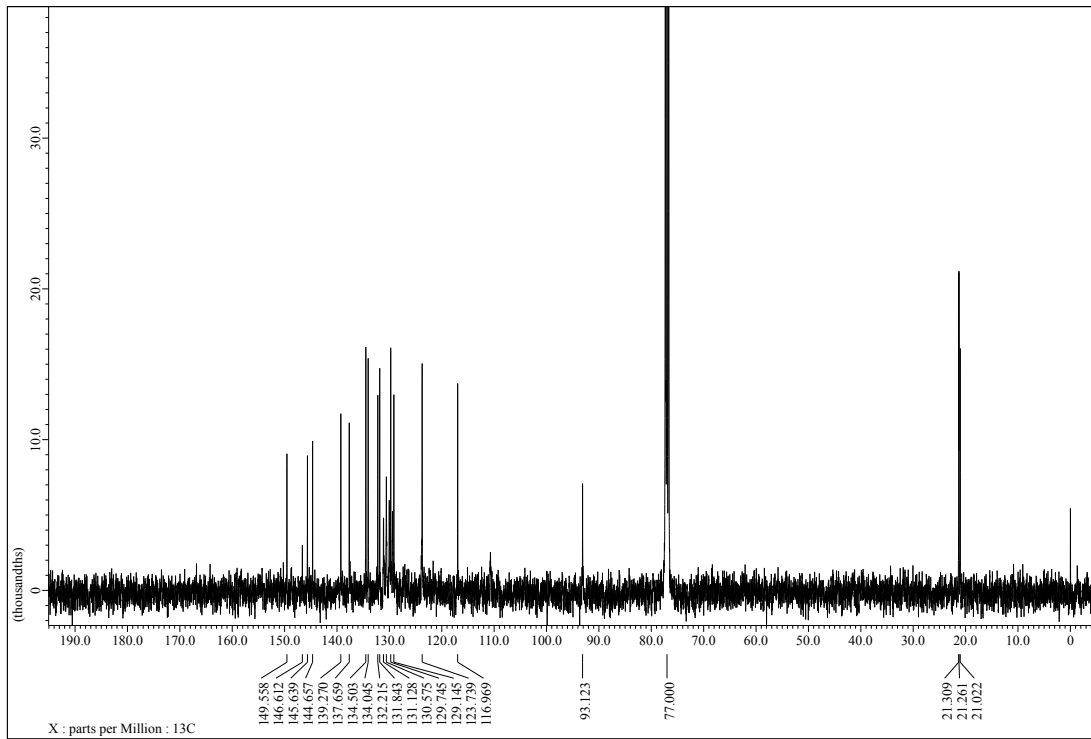


Figure S13. ^{13}C NMR spectrum of **B2** in CDCl_3 at 25 °C.

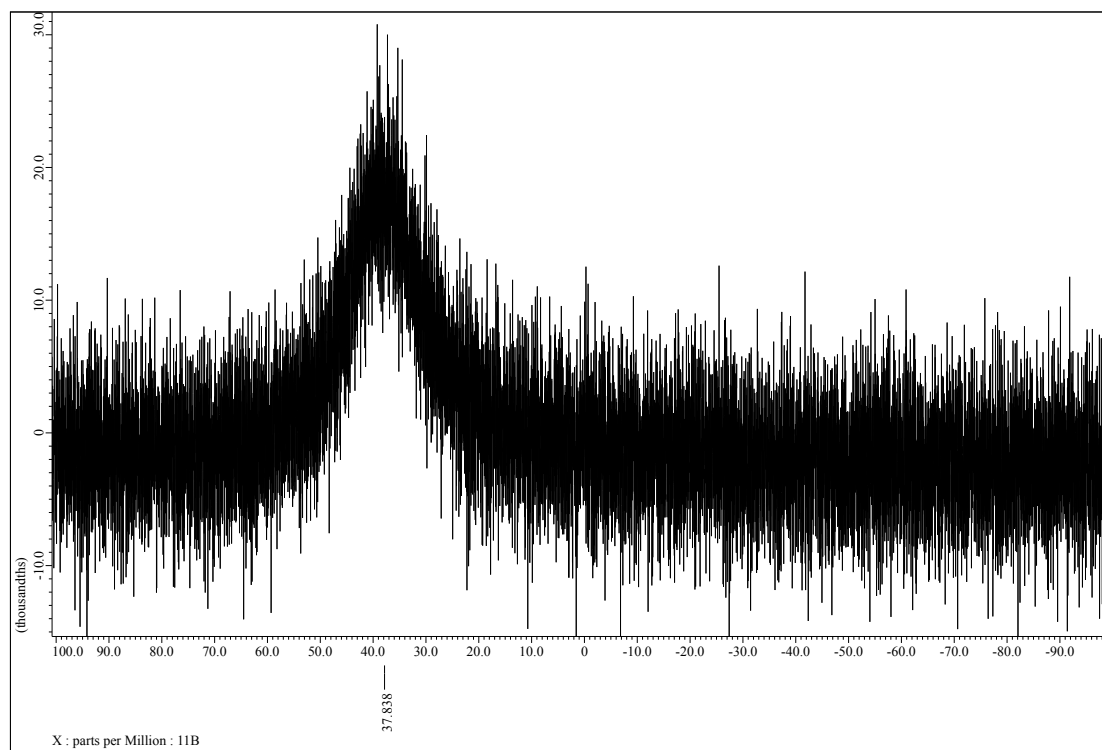


Figure S14. ^{11}B NMR spectrum of **B2** in CDCl_3 at 25 °C.

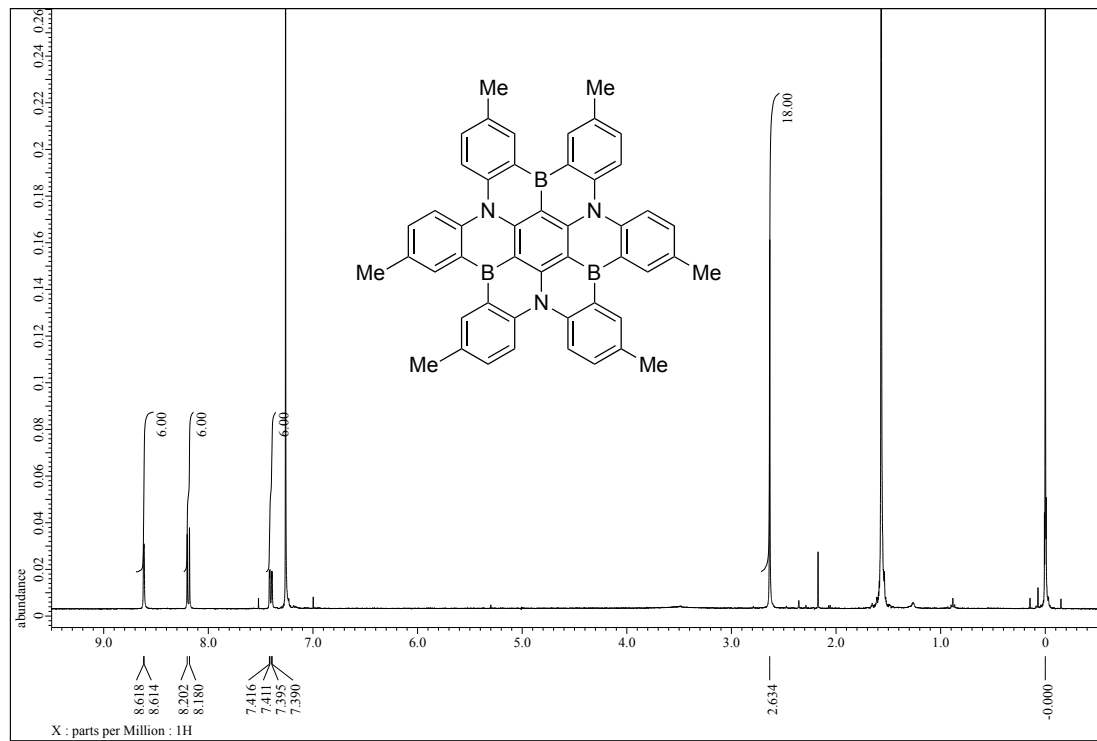


Figure S15. ^1H NMR spectrum of **B3** in $\text{CDCl}_3/\text{CS}_2 = 1/3$ at 25 °C.

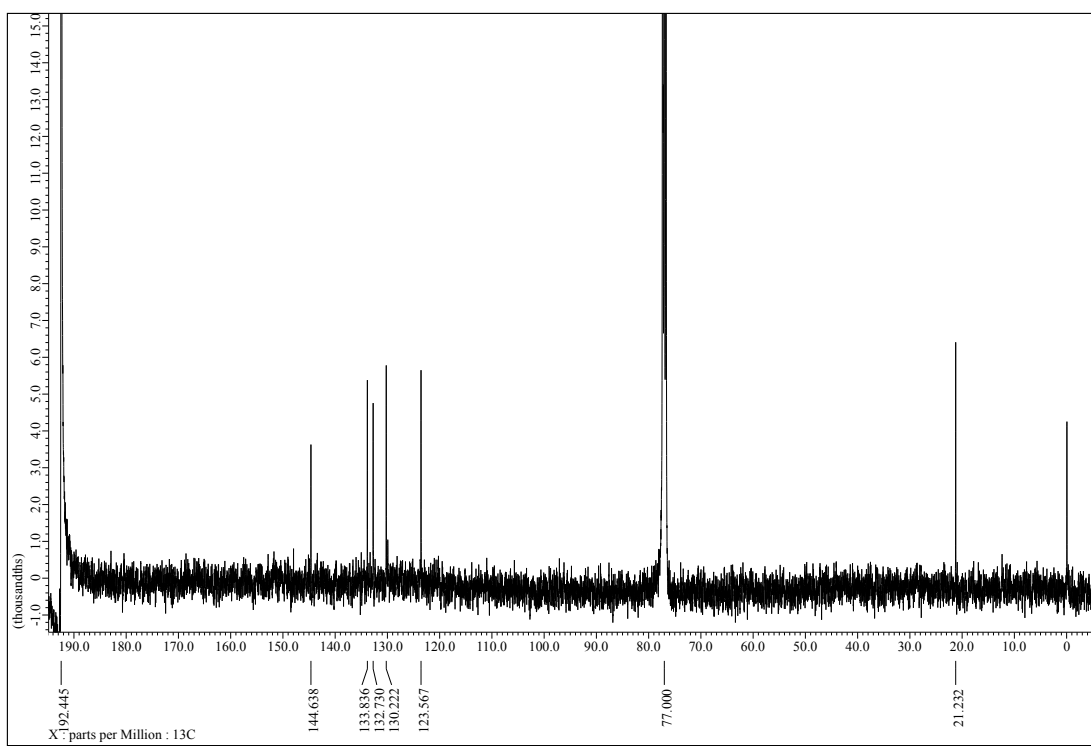


Figure S16. ¹H NMR spectrum of **B3** in CDCl₃/CS₂ = 1/3 at 25 °C.

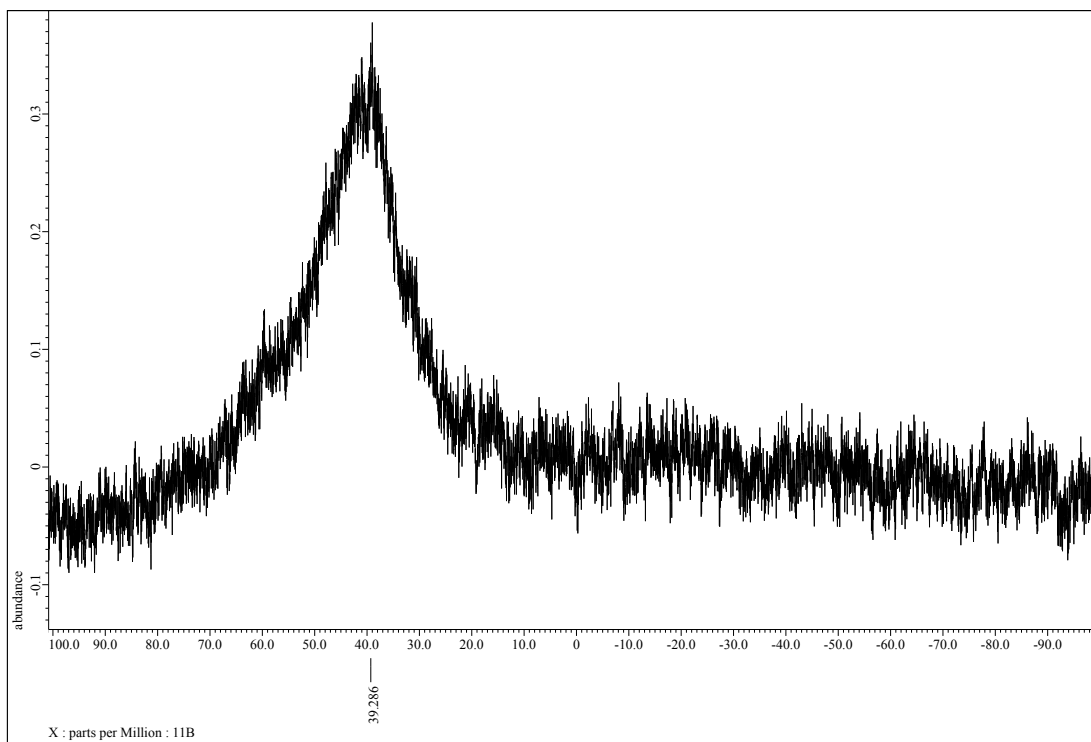


Figure S17. ¹¹B NMR spectrum of **B3** in CDCl₃/CS₂ = 1/3 at 25 °C.

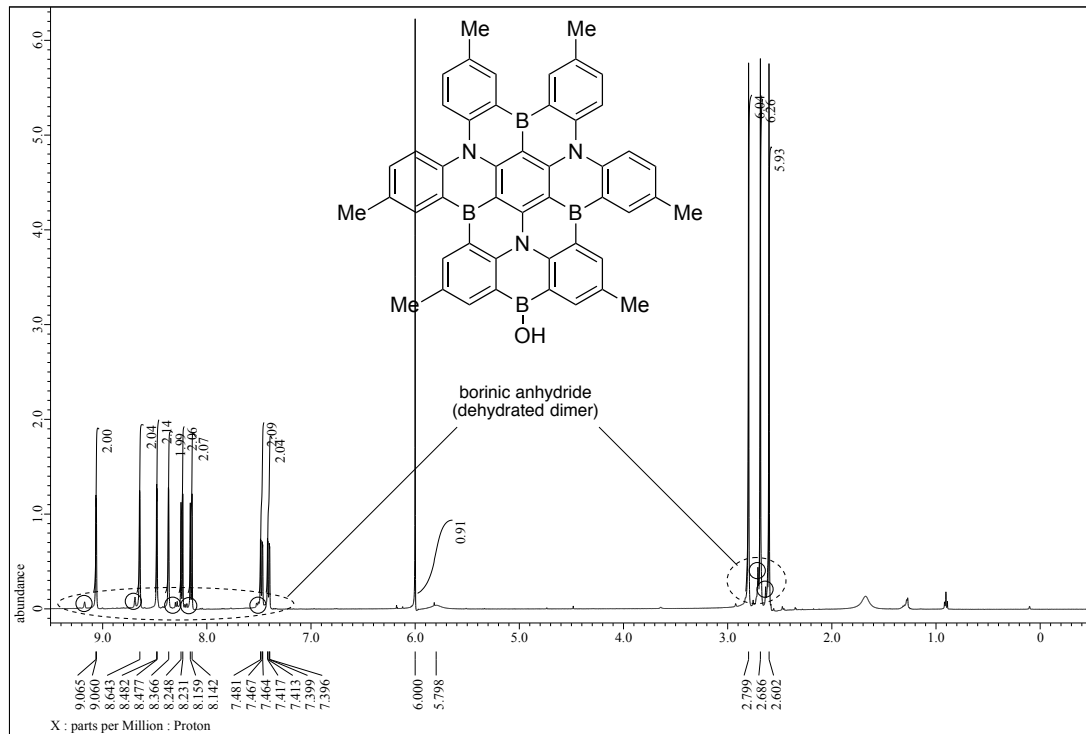


Figure S18. ^1H NMR spectrum of **B4** in $(\text{CDCl}_2)_2$ at 25 °C.

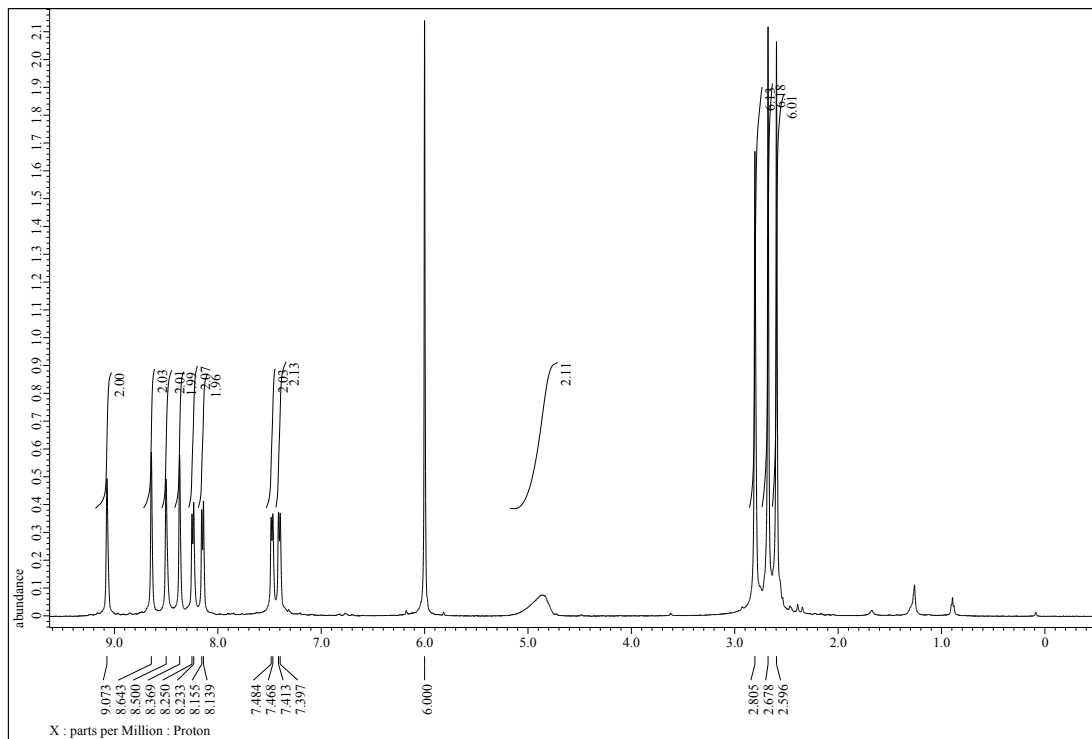


Figure S19. ^1H NMR spectrum of **B4** after hydrolysis in $(\text{CDCl}_2)_2/\text{D}_2\text{O}$ at 25 °C.

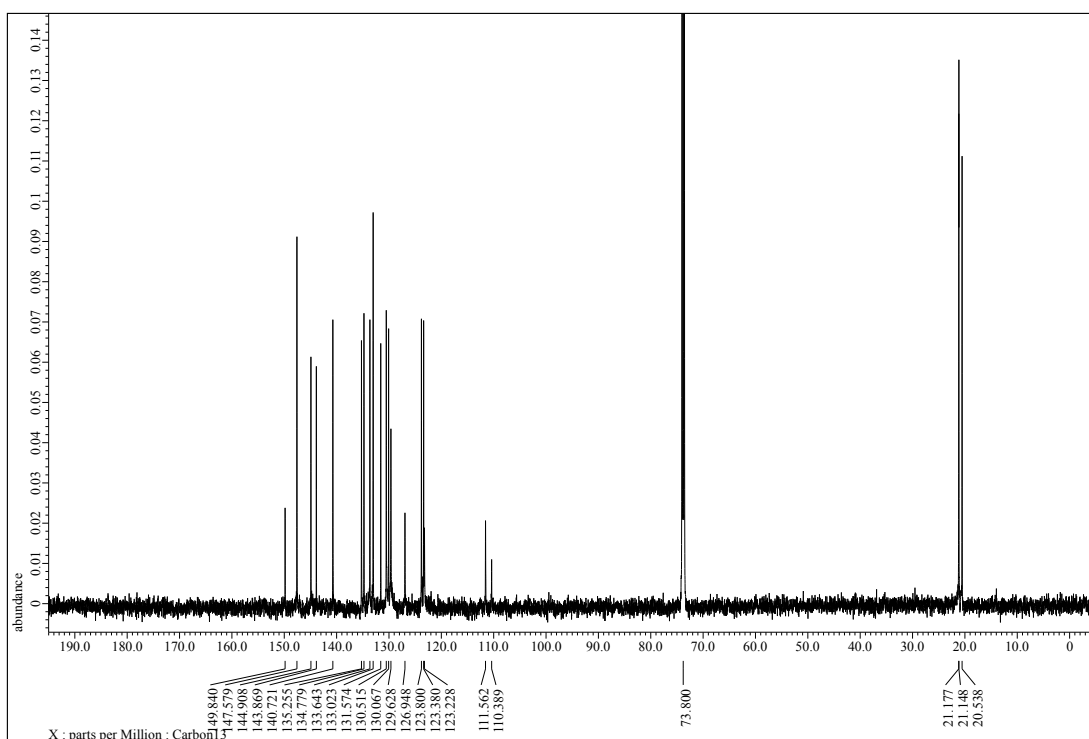


Figure S20. ^{13}C NMR spectrum of **B4** in $(\text{CDCl}_2)_2$ at 60°C .

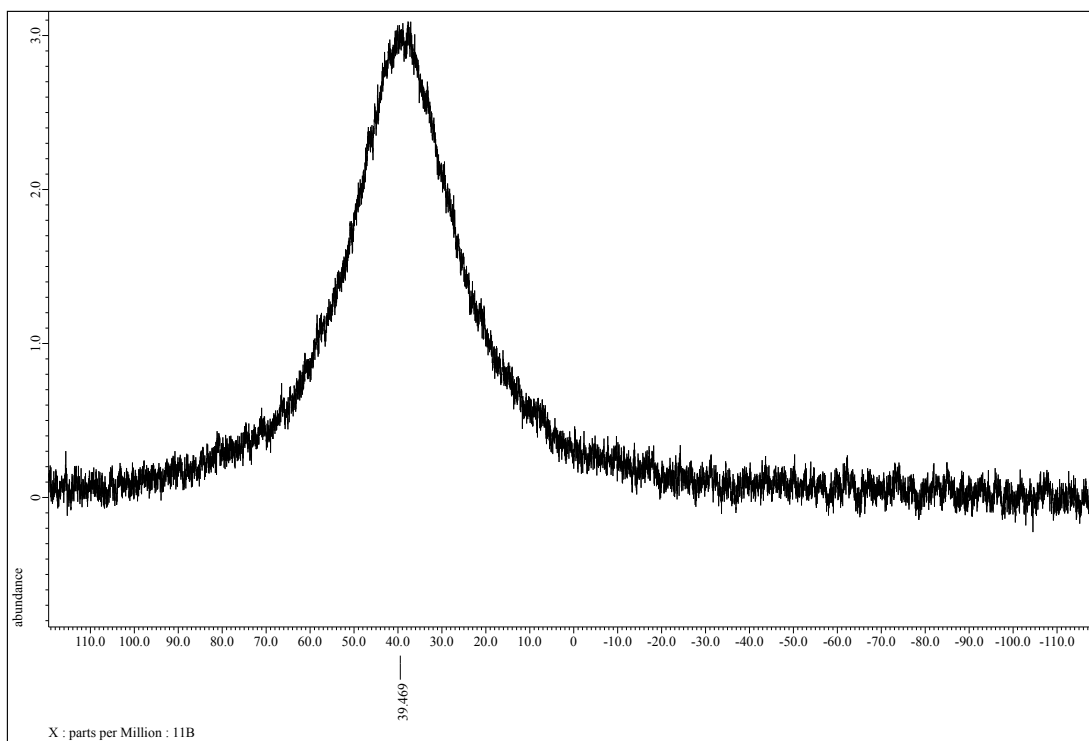


Figure S21. ^{11}B NMR spectrum of **B4** in $(\text{CDCl}_2)_2$ at 25°C .

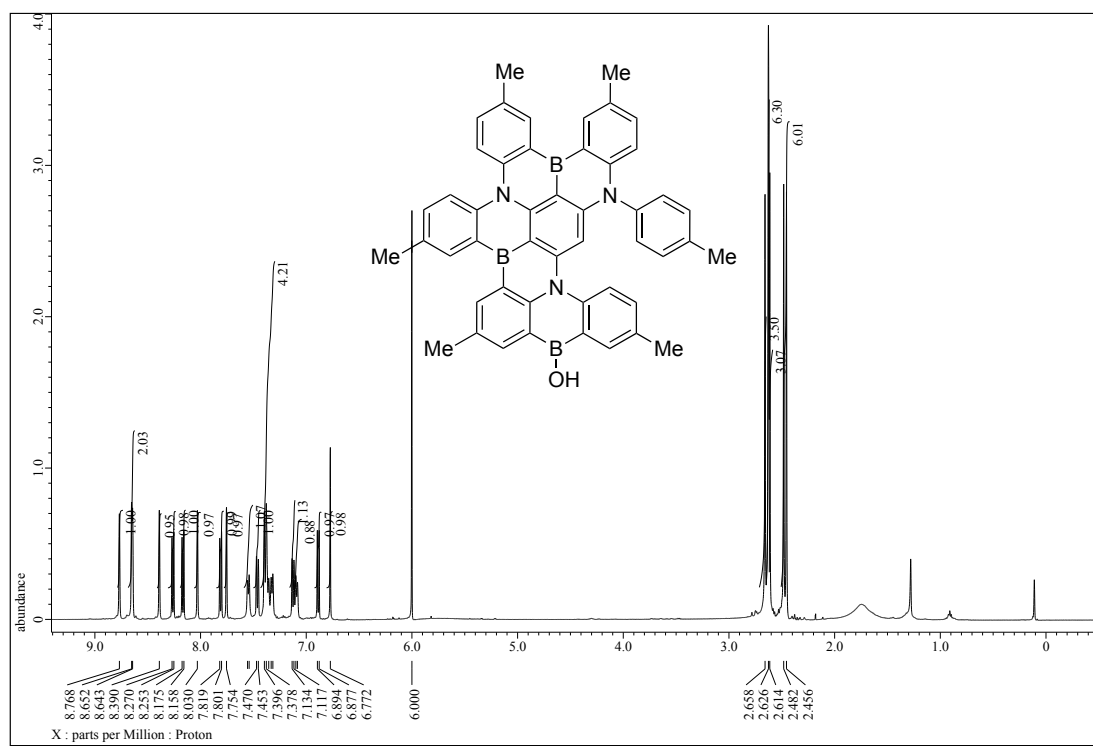


Figure S22. ¹H NMR spectrum of B3-OH in (CDCl₂)₂ at 25 °C.

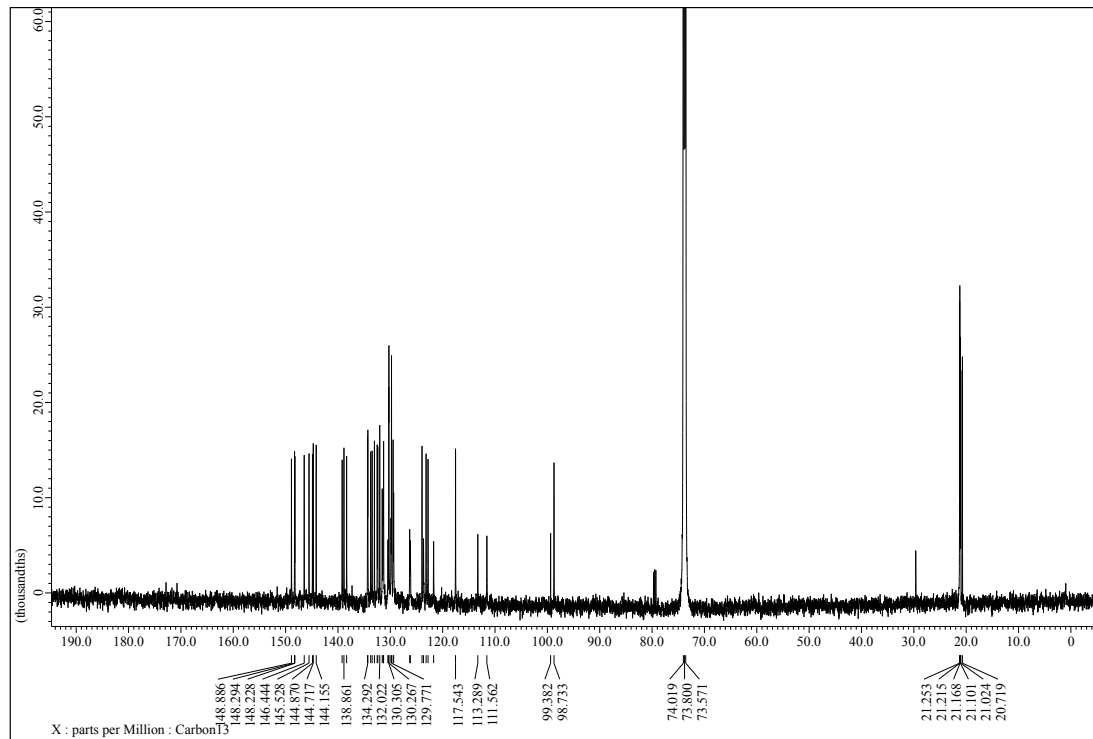


Figure S23. ¹³C NMR spectrum of B3-OH in (CDCl₂)₂ at 60 °C.

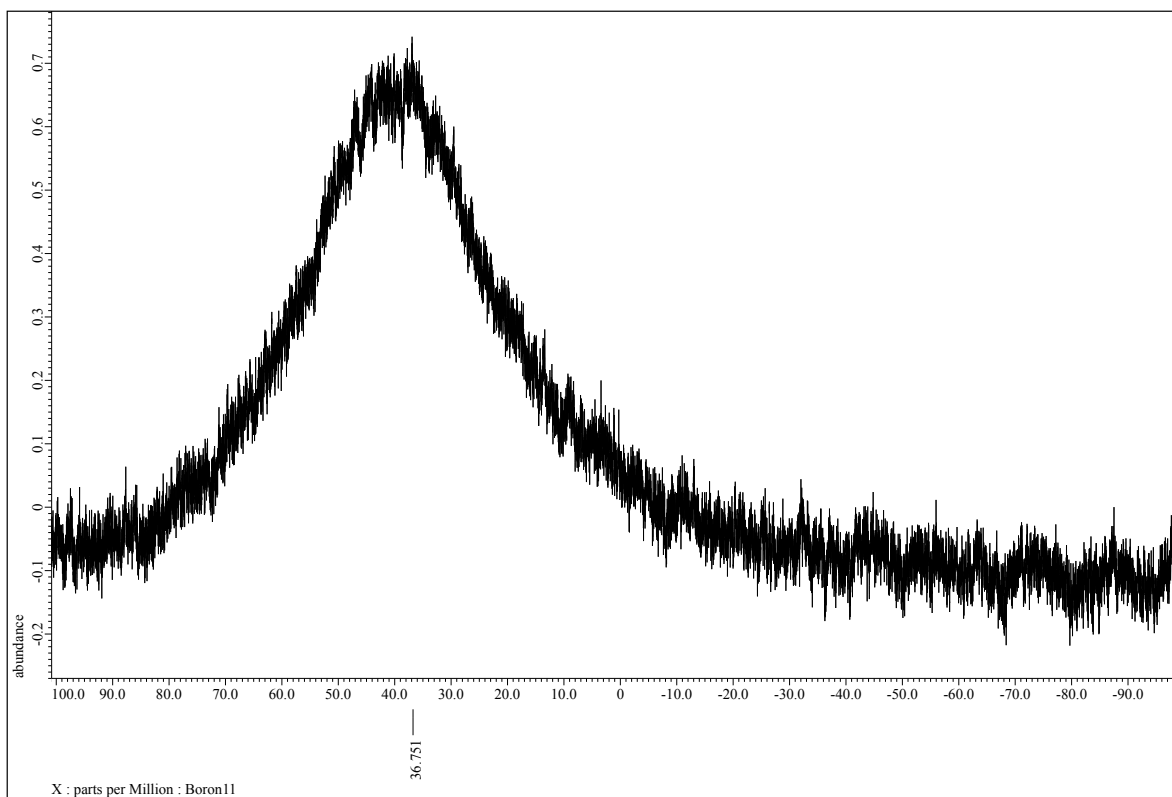
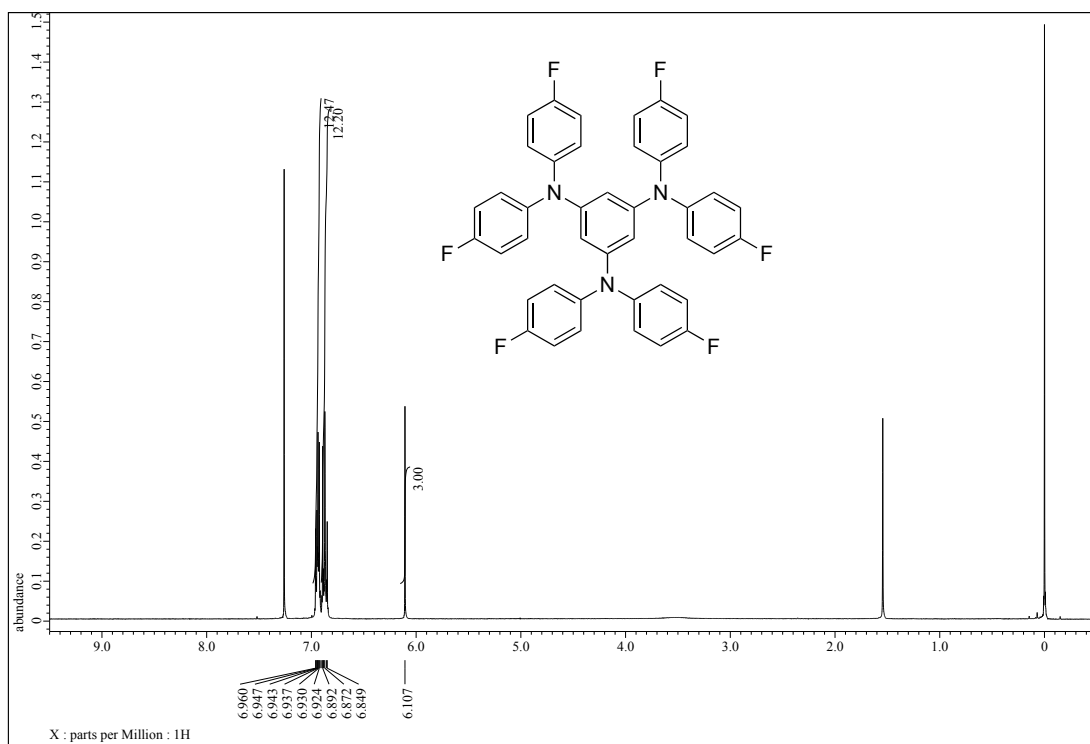


Figure S24. ^{11}B NMR spectrum of **B3-OH** in $(\text{CDCl}_2)_2$ at 25 °C.



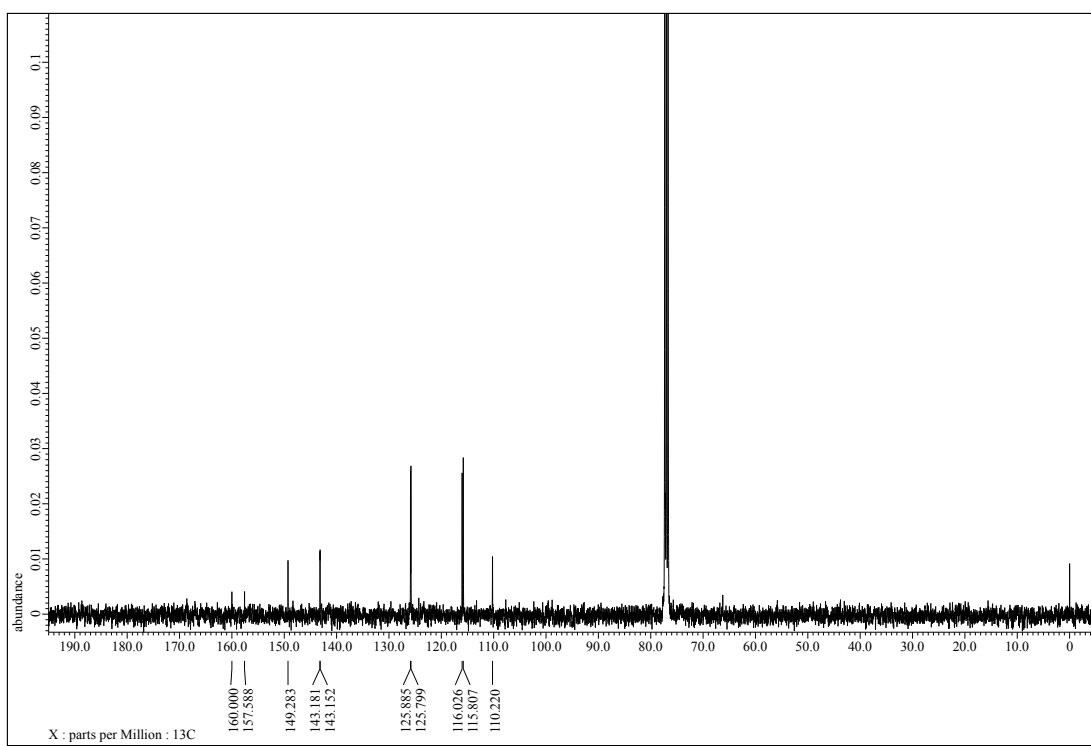


Figure S26. ^{13}C NMR spectrum of **1-F** in CDCl_3 at 25 °C.

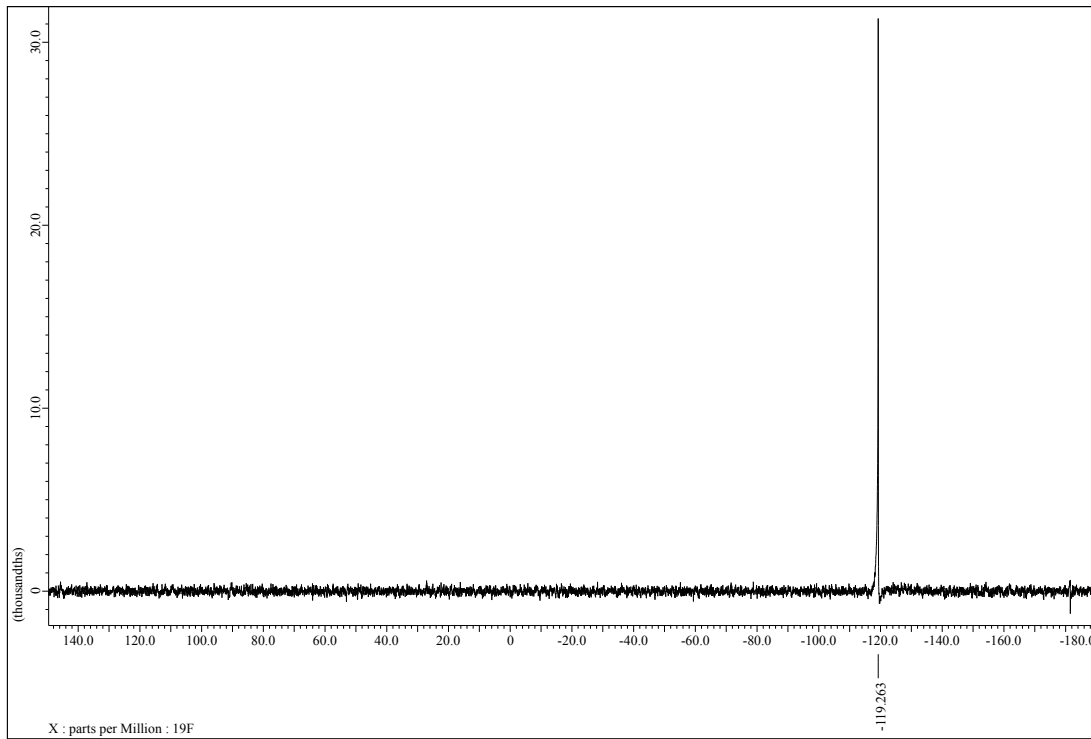


Figure S27. ^{19}F NMR spectrum of **1-F** in CDCl_3 at 25 °C.

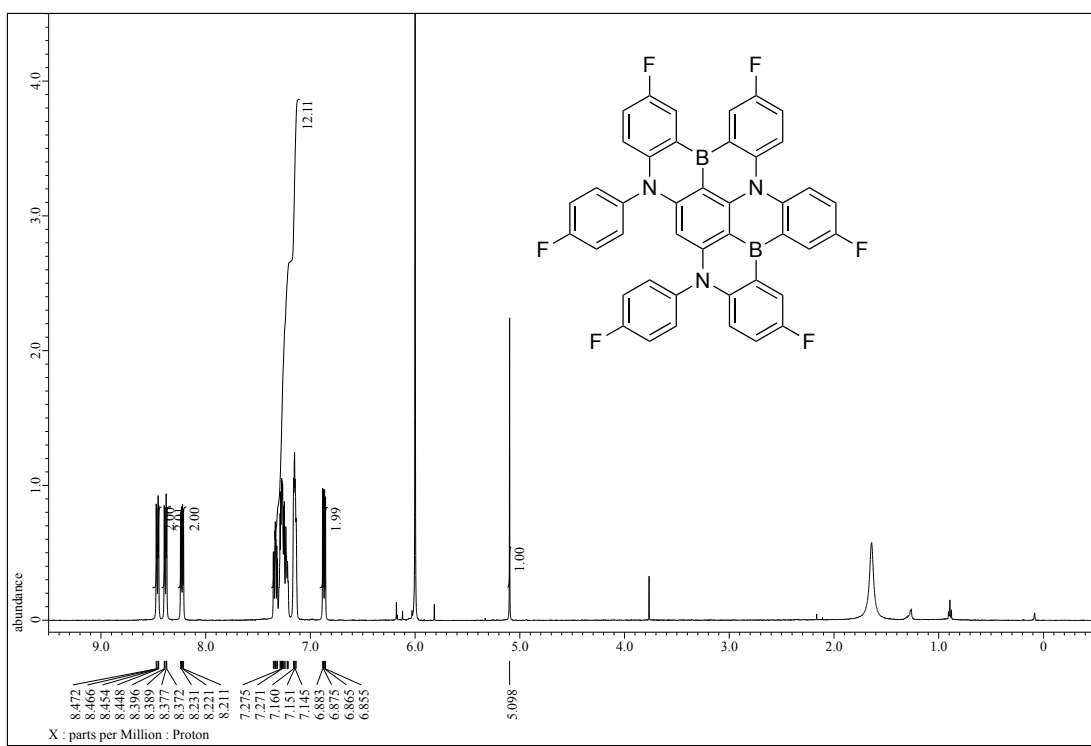


Figure S28. ¹H NMR spectrum of B2-F in (CDCl₂)₂ at 25 °C.

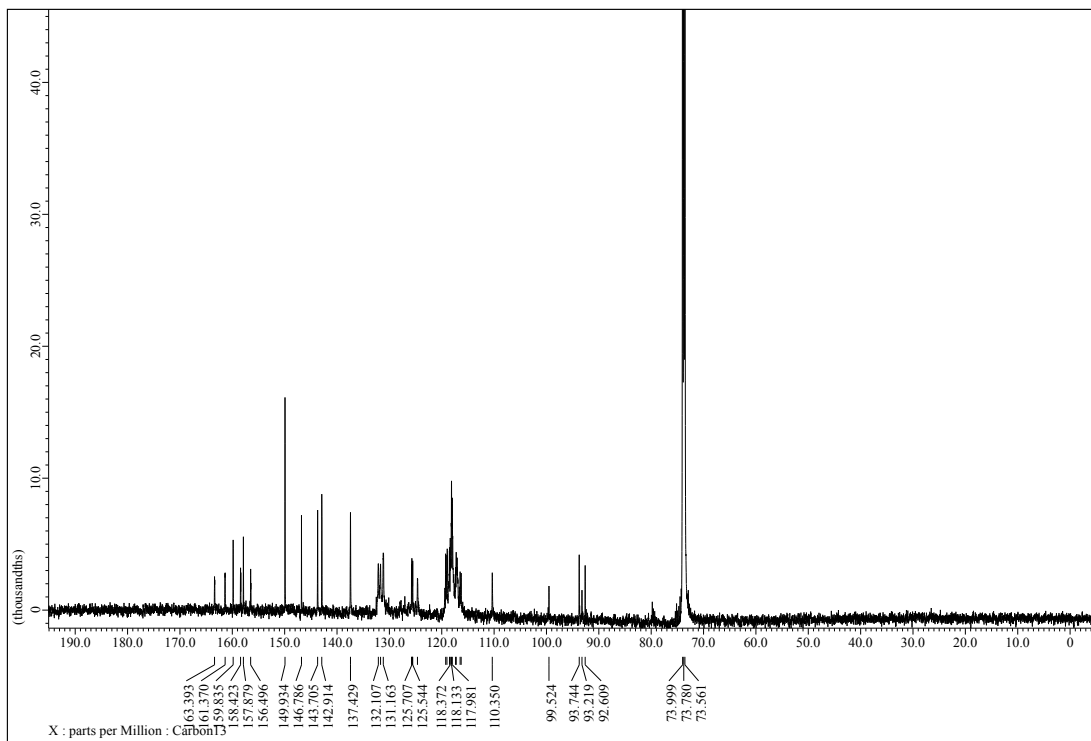


Figure S29. ¹³C NMR spectrum of B2-F in (CDCl₂)₂ at 100 °C.

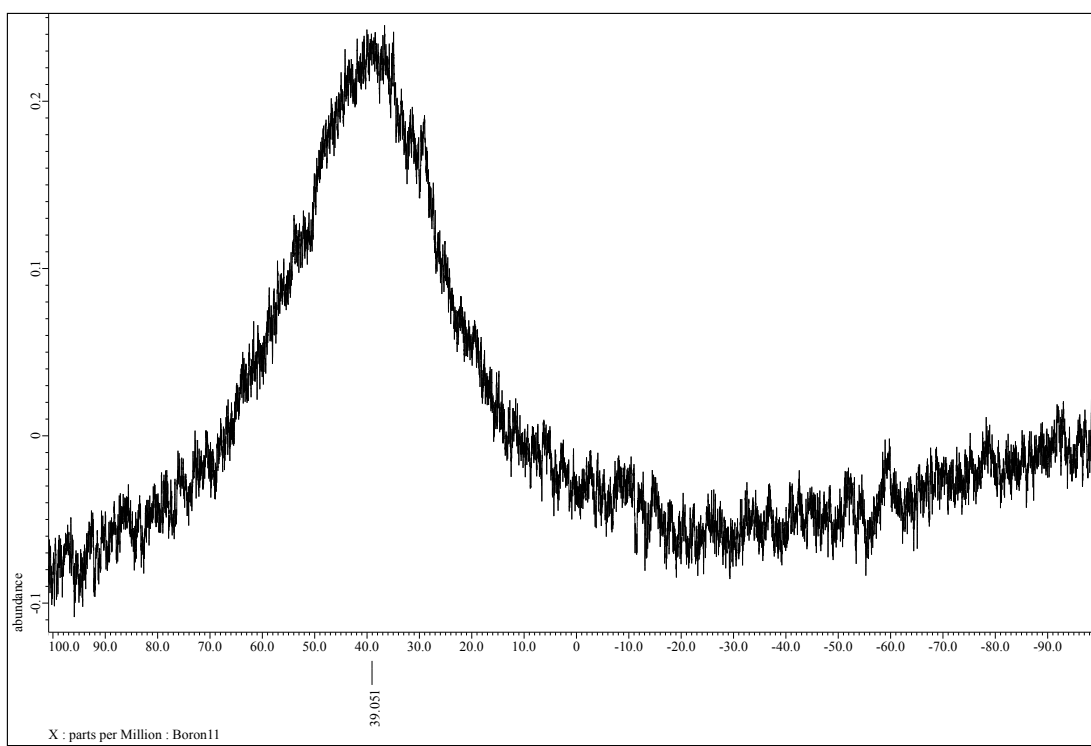


Figure S30. ^{11}B NMR spectrum of **B2-F** in $(\text{CDCl}_2)_2$ at 25 °C.

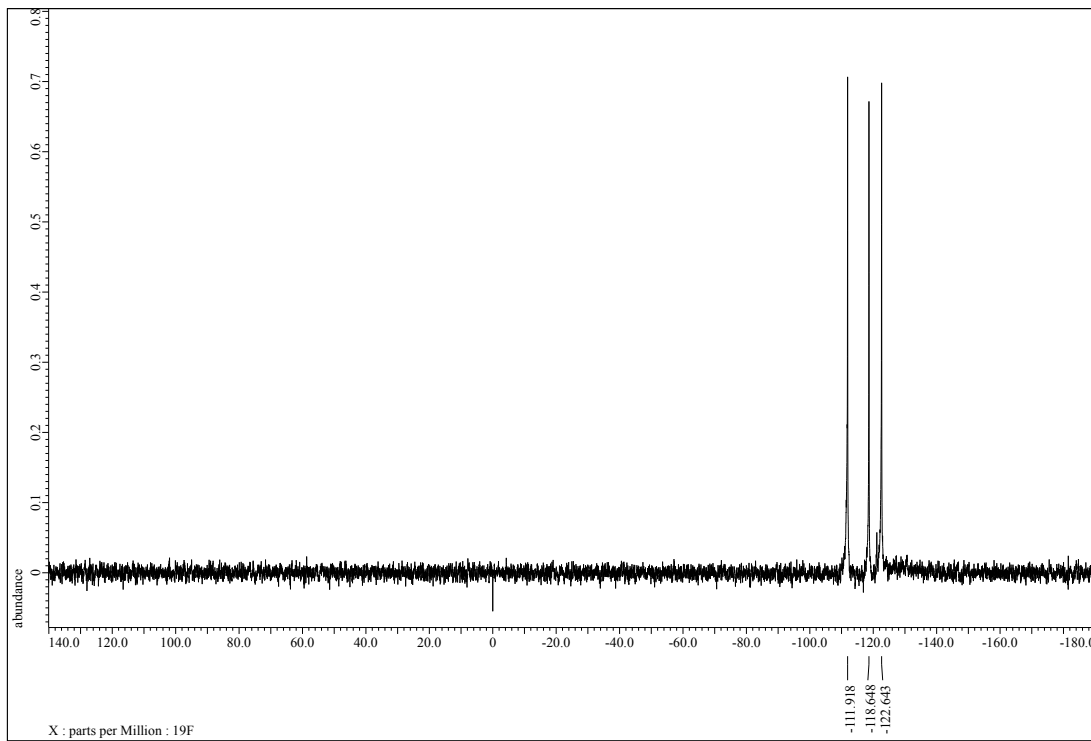


Figure S31. ^{19}F NMR spectrum of **B2-F** in $(\text{CDCl}_2)_2$ at 25 °C.

References

- (1) Still, W. C.; Kahn, M.; Mitra, A. *J. Org. Chem.* **1978**, *43*, 2923–2925.
- (2) Gaussian 09, Revision C.01, Frisch, M. J.; Trucks, G. W.; Schlegel, H. B.; Scuseria, G. E.; Robb, M. A.; Cheeseman, J. R.; Scalmani, G.; Barone, V.; Mennucci, B.; Petersson, G. A.; Nakatsuji, H.; Caricato, M.; Li, X.; Hratchian, H. P.; Izmaylov, A. F.; Bloino, J.; Zheng, G.; Sonnenberg, J. L.; Hada, M.; Ehara, M.; Toyota, K.; Fukuda, R.; Hasegawa, J.; Ishida, M.; Nakajima, T.; Honda, Y.; Kitao, O.; Nakai, H.; Vreven, T.; Montgomery, Jr., J. A.; Peralta, J. E.; Ogliaro, F.; Bearpark, M.; Heyd, J. J.; Brothers, E.; Kudin, K. N.; Staroverov, V. N.; Keith, R.; Kobayashi, R.; Normand, J.; Raghavachari, K.; Rendell, A.; Burant, J. C.; Iyengar, S. S.; Tomasi, J.; Cossi, M.; Rega, N.; Millam, N. J.; Klene, M.; Knox, J. E.; Cross, J. B.; Bakken, V.; Adamo, C.; Jaramillo, J.; Gomperts, R.; Stratmann, R. E.; Yazyev, O.; Austin, A. J.; Cammi, R.; Pomelli, C.; Ochterski, J. W.; Martin, R. L.; Morokuma, K.; Zakrzewski, V. G.; Voth, G. A.; Salvador, P.; Dannenberg, J. J.; Dapprich, S.; Daniels, A. D.; Farkas, Ö.; Foresman, J. B.; Ortiz, J. V.; Cioslowski, J.; Fox, D. J. Gaussian, Inc., Wallingford CT, 2010.
- (3) (a) Becke, A. D. *J. Chem. Phys.* **1993**, *98*, 5648–5652. (b) Lee, C.; Yang, W.; Parr, R. G. *Phys. Rev. B* **1988**, *37*, 785–789.
- (4) Hehre, W. J.; Radom, L.; Schleyer, P. v. R.; Pople, J. A. *Ab Initio Molecular Orbital Theory*; John Wiley & Sons: New York, 1986 and references cited therein.
- (5) (a) Casida, M. E.; Jamorski, C.; Casida, K. C.; Salahub, D. R. *J. Chem. Phys.* **1998**, *108*, 4439–4449.
(b) Stratmann, R. E.; Scuseria, G. E.; Frisch, M. J. *J. Chem. Phys.* **1998**, *109*, 8218–8224.
- (6) (a) Dichtfield, R. *Mol. Phys.* **1974**, *27*, 789–807. (b) Wolinski, K.; Hinton, J. F.; Pulay, P. *J. Am. Chem. Soc.* **1990**, *112*, 8251–8260.
- (7) Ishikawa, W.; Inada, H.; Nakano, H.; Shirota, Y. *Mol. Cryst. Liq. Cryst.* **1992**, *211*, 413–438.
- (8) Messerschmidt, A.; Schneider, M.; Huber, R. *J. Appl. Cryst.* **1990**, *23*, 436.
- (9) Burla, M. C.; Caliandro, R.; Camalli, M.; Carrozzini, B.; Cascarano, G. L.; De Caro, L.; Giacovazzo, C.; Polidori, G.; Spagna, R. *J. Appl. Cryst.* **2005**, *38*, 381.
- (10) Burla, M. C.; Caliandro, R.; Camalli, M.; Carrozzini, B.; Cascarano, G. L.; De Caro, L.; Giacovazzo, C.; Polidori, G.; Siliqi, D.; Spagna, R. *J. Appl. Cryst.* **2007**, *40*, 609.
- (11) Sheldrick, G. M. *Acta Crystallogr. Sect. A* **2008**, *A64*, 112.
- (12) Masui, K.; Nakanotani, H.; Adachi, C. *Org. Electron.* **2013**, *14*, 2721.
- (13) Zhang, Q.; Kuwabara, H.; Potscavage, W. J.; Huang, S.; Hatae, Y.; Shibata, T.; Adachi, C. *J. Am. Chem. Soc.* **2014**, *136*, 18070–18081.
- (14) H. Kaji, H. Suzuki, T. Fukushima, K. Shizu, K. Katsuaki, S. Kubo, T. Komino, H. Oiwa, F. Suzuki, A. Wakamiya, Y. Murata, C. Adachi, *Nat. Commun.* **2015**, *6*, 8476.